

Mass Measurements of Stellar and Intermediate-Mass Black-Holes

J. Casares · P.G. Jonker

Received: date / Accepted: date

Abstract We discuss the method, and potential systematic effects therein, used for measuring the mass of stellar-mass black holes in X-ray binaries. We restrict our discussion to the method that relies on the validity of Kepler's laws; we refer to this method as the dynamical method. We briefly discuss the implications of the mass distribution of stellar-mass black holes and provide an outlook for future measurements. Further, we investigate the evidence for the existence of intermediate-mass black holes i.e. black holes with masses above $100 M_{\odot}$, the limit to the black hole mass that can be produced by stellar evolution in the current Universe.

Keywords Black holes · X-ray binaries · accretion disks

1 Introduction

Black holes (BH) are the pinnacle of extreme gravity. They provide astronomers with unique laboratories for observing some of the most fundamental and intriguing astrophysical phenomena, such as accretion, the ejection of relativistic outflows or the production of gamma-ray bursts. Consequently, BHs play an essential role in a variety of astrophysical phenomena on various scales, ranging from binaries to ultra-luminous X-ray sources (ULXs), galaxies and quasars, the most powerful accretion engines in the Universe. However, it is *stellar-mass* BHs that offer us the best opportunity to study these objects in detail. Their proximity and variability time scales allow in-depth studies of their properties through a range of accretion regimes on time-scales convenient for study by humans. Thorough reviews on BH accretion and outflows are given in several other articles of this issue.

J. Casares

Instituto de Astrofísica de Canarias, E-38205 La Laguna, S/C de Tenerife, Spain
Departamento de Astrofísica, Universidad de La Laguna, E-38206 La Laguna, S/C de Tenerife, Spain E-mail: jorge.casares@iac.es

P.G. Jonker

SRON, Netherlands Institute for Space Research, Sorbonnelaan 2, 3584 CA, Utrecht, The Netherlands
Department of Astrophysics/IMAPP, Radboud University Nijmegen, P.O. Box 9010, 6500 GL, Nijmegen, The Netherlands
Harvard-Smithsonian Center for Astrophysics, 60 Garden Street, Cambridge, MA 02138, U.S.A.

Astrophysical BHs are characterized by only two parameters, mass and spin, and their knowledge is key to probe space-time in the strong gravity regime (see articles by McClintock et al. and Reynolds in this issue). Accurate knowledge of BH masses is also critical to test models of massive progenitors, SNe Ibc explosions and compact binary evolution (e.g. Fryer & Kalogera 2001; Fryer et al. 2012; Belczynski et al. 2012). The current article presents an up-to-date overview of dynamical mass determinations in stellar-mass BHs. The main methods of analysis are summarized, together with a critical assessment on their limitations and possible systematics involved. In a second part of the article, new approaches and techniques are reviewed from which a significant advance in the precision of mass measurements is expected. Finally, a section on prospects for mass determination in ULXs is presented. Previous reviews on observational properties and mass determination in BH binaries can be found in van Paradijs & McClintock (1995), Tanaka & Shibazaki (1996), Orosz (2003), Charles & Coe (2006), Remillard & McClintock (2006), McClintock & Remillard (2006), Casares (2007) and Belloni et al. (2011).

2 Dynamical BHs in X-ray Transients

Stellar evolution predicts $\gtrsim 10^8$ BH remnants in the Galaxy (van den Heuvel 1992) but only BHs in compact binaries can be easily detected through accretion. X-ray binaries thus provide currently the best way to measure the mass of BHs. A large number of these X-ray binaries are found as X-ray transients (XRTs, for a comprehensive review see McClintock & Remillard 2006). XRTs are singled out by episodic outbursts caused by mass transfer instabilities in an accretion disc which is fed by a low-mass (donor) star (Mineshige & Wheeler 1989; Lasota 2001). The large fraction of BH systems among XRTs agrees with the predictions of the Disc Instability Model, modified by irradiation effects. The absence of a solid surface in the compact star inhibits disc stabilization through X-ray irradiation at the low accretion rates characteristic of overflowing low-mass stars (King et al. 1997; Coriat et al. 2012). XRTs may increase the integrated X-ray luminosity of the Milky Way by a factor ~ 2 and thus are promptly spotted by X-ray satellites. Between outbursts, they remain in a "quiescent" state, with typical X-ray luminosities below $\sim 10^{32}$ erg s $^{-1}$, allowing the optical detection of the faint low-mass donor star. This opens-up the possibility to perform radial velocity studies, probe the nature of the compact star and determine its mass.

The most robust method of measuring stellar masses relies on Kepler's Third law of motion. However, BH X-ray binaries are akin to single-lined spectroscopic binaries and hence only the radial velocity curve of the mass-losing star is available (Fig. 1). This yields the orbital period P_{orb} and the radial velocity semi-amplitude of the companion star K_c . The two quantities combine in the mass function equation $f(M)$, a non-linear expression relating the masses of the compact object M_x and the companion star M_c (or binary mass ratio $q = M_c/M_x$) with the binary inclination angle (i):

$$f(M) = \frac{K_c^3 P_{\text{orb}}}{2\pi G} = \frac{M_x^3 \sin^3 i}{(M_x + M_c)^2} = \frac{M_x \sin^3 i}{(1 + q)^2} \quad (1)$$

Note that this expression implicitly assumes orbits are circular, which is a fair assumption given the long lifetimes and short circularization timescales expected in X-ray binaries (Witte & Savonije 2001). The mass function provides a solid lower limit to the mass of the compact star for $M_c = 0$ and an edge-on geometry ($i = 90^\circ$). A large mass function is widely considered as the best signature for a BH since observations and theoretical calculations of dense matter indicate that neutron stars cannot be more massive than $\sim 2.5 M_\odot$ (Lattimer

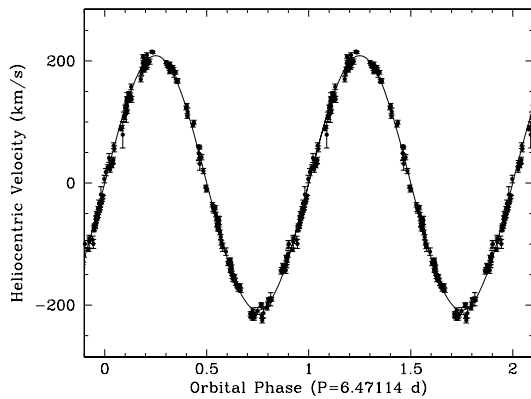


Fig. 1 Radial velocity curve of the K0 donor star in the XRT V404 Cyg.

2012). Besides, main sequence stars with masses above $\sim 3 M_{\odot}$ would be B-type stars, and would be seen in the spectra. The fact that only a K/M-type stellar spectrum is detected together with the presence of an occasionally very bright X-ray source leads to the conclusion that the binary contains a BH.

The radial velocity curve of the donor star is best obtained through cross-correlation of the photospheric absorption lines with a stellar template of similar spectral type. Mass functions are gathered routinely to a few percent accuracy and this requires resolving powers better than about $\lambda/\Delta\lambda=1500$. The use of 10 m class telescopes has allowed one to measure $f(M)$ for objects down to $R\sim 22$ mag, as shown by the works on XTE J1859+226 (Filippenko & Chornock 2001; Corral-Santana et al. 2011). BH mass measurements require also the measurement of the mass ratio q and the binary inclination which, in the absence of eclipses, can only be obtained through indirect methods. These are based on information to be extracted from the *light curve* and the *spectrum* of the optical star, resulting in a full solution to the binary parameters with minimum assumptions. This procedure will be discussed in turn.

The best way to determine the mass ratio is through measuring the rotational broadening ($V \sin i$) of the photospheric lines from the companion star. This technique exploits the fact that the star fills its Roche lobe and it is tidally locked. This makes the absorption lines significantly broader than in single stars that are slowly rotating. Under the approximation of sphericity, the rotational broadening scales with the velocity of the donor star according to $V \sin i/K_c \simeq 0.462 q^{(1/3)}(1+q)^{(2/3)}$ (Wade & Horne 1988) and hence q can be constrained. The rotational broadening is usually measured by comparing the target spectrum with a slowly rotating template, convolved with a limb-darkened rotational profile (e.g. Gray 1992). A χ^2 minimization yields the optimum broadening required by the template to match the spectrum of the companion to the BH (see Fig. 2). Typical rotational broadenings in BH transients range between 30 and 120 km s^{-1} and thereby moderately high spectral resolutions ($\lambda/\Delta\lambda \gtrsim 5000$) are required for these measurements otherwise erroneous values for $V \sin i$ are likely obtained.

It should be noted that there are systematic errors involved in the calculation of $V \sin i$. First of all, Roche-lobe-filling stars are obviously non-spherical, with tidal distortion caus-

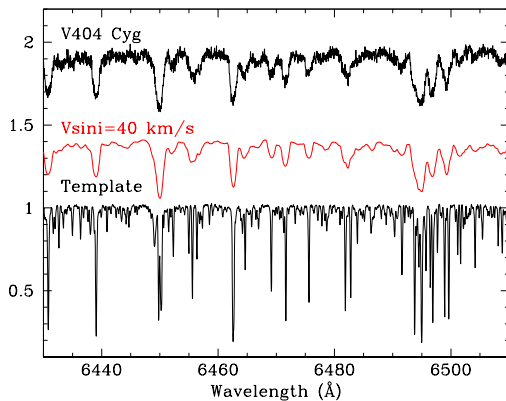


Fig. 2 Rotational broadening analysis. A KOIV template star (bottom) is broadened by $V \sin i = 40 \text{ km s}^{-1}$ (middle) in order to reproduce the spectrum of the donor star in the BH transient V404 Cyg (top). The latter has been produced after coadding individual spectra in the rest frame of the companion star.

ing orbital variations of the broadening kernel. Fitting the phase-averaged spectrum with a template broadened using a spherical convolution profile yields $V \sin i$ values which underestimate q (Marsh, Robinson & Wood 1994). In addition, the use of a continuum limb-darkening approximation also leads to underestimates of the true broadening and thus a decreased mass ratio (Shahbaz 2003). Another potential source of systematics is introduced by assuming a gravity darkening law described by von Zeipel’s theorem with exponent $\beta = 0.08$ (Lucy 1967, but see Sarna 1989). In any case, statistical uncertainties in the computation of $V \sin i$ are typically larger than systematic errors and hence mass ratios obtained through measuring rotational broadenings are, in most cases, robust. Furthermore, given the extreme mass ratios ($q \ll 1$) typical of BH XRTs, the impact of q uncertainties in the final BH mass is modest.

The binary inclination is commonly obtained through fitting optical/NIR light curves with synthetic ellipsoidal models. Light curves in XRTs show a characteristic double-humped modulation produced by the tidal distortion of the Roche lobe filling donor star and a non-uniform distribution of surface brightness. The amplitude of the modulation is a strong function of the inclination angle. Synthetic models are computed integrating the local flux intensity, modified by limb and gravity darkening effects, over the Roche geometry. The best results are obtained using Kurucz and NEXTGEN model atmospheres (see Orosz & Hauschildt 2000 for a critical comparison of several approaches). For example, Fig. 3 presents a textbook example of the ellipsoidal modulation from GRO J1655-40, an XRT with a F6IV intermediate-mass donor star. Synthetic model fits performed by different groups have resulted in very accurate inclination values distributed over a narrow range between $64\text{--}71^\circ$ (Orosz & Bailyn 1997; van der Hooft et al. 1998; Greene et al. 2001; Beer & Podsiadlowsky 2002). However, the vast majority of XRTs possess faint K-M donor stars and, therefore, light curves can be seriously contaminated by other non-stellar sources of light. The impact of these on the determination of inclination angles and BH masses can be critical and will be discussed in Section 2.1.

Table 1 presents a compilation of fundamental parameters and BH mass determinations for the 17 BH XRTs with dynamical confirmation currently known. Uncertainties are typically $1\text{-}\sigma$ except for errors in the inclination angle where a 90 or 95 percent confidence level

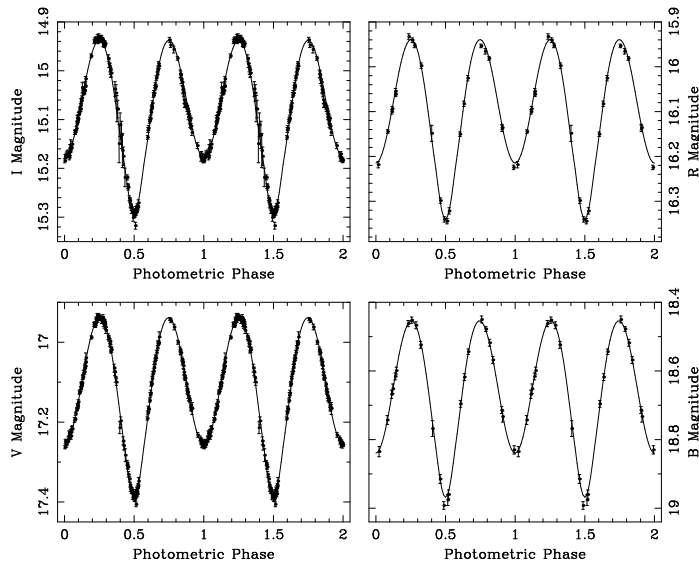


Fig. 3 Ellipsoidal fits to light curves of the XRT GRO J1655-40 in four colour bands simultaneously. Synthetic models were computed using Kurucz model atmospheres. From Beer & Podsiadlowsky (2002).

is sometimes provided. The mass functions listed in the table have been obtained from radial velocity curves of the companion stars in quiescence, with the exception of GX 339-4 (see also footnotes on GRS 1915+105 and GRO J1655-40). In the case of GX 339-4, the donor star has not been detected in quiescence yet, although a lower limit to the mass function was derived using emission lines, excited on its irradiated hemisphere during an outburst episode (Hynes et al. 2003a; see Section 4.1). Table 1 also quotes mass ratios obtained exclusively through the $V \sin i$ technique, besides that from GRO J1655-40 where its high mass ratio also allows one to constrain q from model fits to the ellipsoidal light curves. Finally, binary inclinations refer to values derived from modelling ellipsoidal light curves in quiescence, except for GRS 1915+105, where it has been inferred from the orientation of the radio jets (Fender et al. 1999). In some cases, upper limits to the inclinations are given, based on the lack of X-ray eclipses and mass ratio constraints. Numbers highlighted in boldface indicate our recommended set of fundamental parameters to be adopted. In our view, these provide the best determinations currently available i.e. those least affected by possible systematic effects and having the lowest statistical uncertainties.

2.1 Systematic errors and biases in BH mass determinations

The error bars on BH mass measurements are dominated by uncertainties in the inclination angle because of its cubic dependence in equation 1. But most worryingly, Table 1 indicates that ellipsoidal fits performed by independent groups on the same binary often lead to a wide spread of inclinations and thereby BH masses. This is mainly thought to be due to systematic effects caused by contamination from non-stellar sources of light rather than statistical errors. There are two main sources of systematics affecting light curve analysis. The first one is the presence of a *superhump* modulation, a distorting wave produced by an eccentric disc precessing with a timescale a few percent longer than the orbital period. Su-

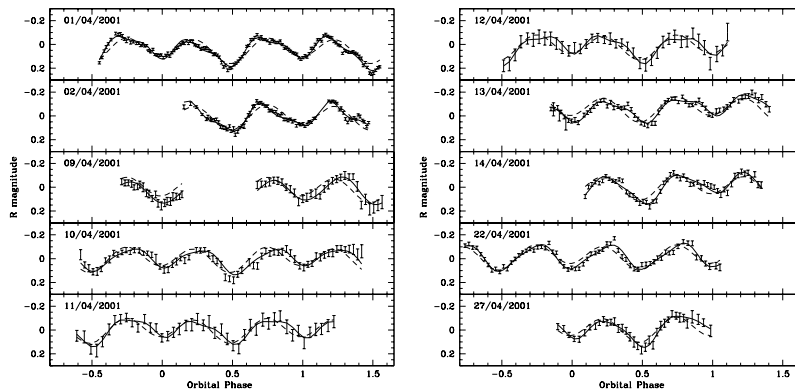


Fig. 4 Ellipsoidal light curves distorted by a superhump in XTE J1118+480. A combined model of an ellipsoidal plus superhump waves (continuous line) provides a better description of the data than a pure ellipsoidal fit (dashed line). From Zurita et al. (2002).

perhumps are typically seen in outburst, when the accretion disc exceeds the 3:1 resonance radius (O’Donoghue & Charles 1996), but can also be detected near quiescence. When this happens, the ellipsoidal light curve is distorted by secular changes in shape and relative height of the maxima and minima (Fig. 4). Intensive monitoring over several orbital cycles is thus important to disentangle potential superhump waves from the true ellipsoidal modulation. Sometimes asymmetries in ellipsoidal light curves are interpreted as contamination by a hot spot (when extra flux is located at phase ~ 0.75 , e.g. Khargharia et al. 2013) or stellar spots. Observations of sharp asymmetries in the light curves can also be mistaken for eclipse features, leading to overestimates in the inclination angle (Haswell et al. 1993).

The second source of systematics is caused by contamination from rapid aperiodic variability. The presence of optical flares in V404 Cyg, with a timescale of ~ 6 hr, was already noticed long ago but thought to be peculiar to this system (Wagner et al. 1992; Pavlenko et al. 1996). However, subsequent high-time resolution (1-5 mins) light curves have revealed that all quiescent XRTs display the same type of variability, with typical amplitudes ranging from 0.06 to 0.6 mag (Zurita et al. 2003; Hynes et al. 2003b; see Fig. 5 but also Shahbaz et al. 2013 for a record ~ 1.5 mag amplitude flaring activity). The variability seems stronger for systems with cooler companions and its characteristic time-scale appears to increase with orbital period, both properties suggesting an accretion disc origin. Magnetic reconnection events (Zurita et al. 2003), X-ray reprocessing (Hynes et al. 2004), instabilities in the transition between the thin and advective disc (Shahbaz et al. 2003) and variable synchrotron emission from a disc jet/outflow (Shahbaz et al. 2013) have been proposed but the physical mechanism responsible for the rapid variability is still unknown.

It is commonly assumed that the accretion disc light follows a negative power law with λ (see Table 1 in Garcia et al. 1996) and thereby most ellipsoidal fits tend to be performed at NIR wavelengths to minimize contamination. However, strong flaring activity is also observed in several NIR light curves, questioning this strategy. The most dramatic case is presented by K-band observations of GRO J0422+320, where the ellipsoidal modulation becomes completely diluted by the flaring variability (Reynolds et al. 2007). Further, flickering is not a white noise process (the PDS is described by a negative power-law with index ~ -1.3 , see Shahbaz et al. 2003) and thus it is not cancelled out after binning or averaging

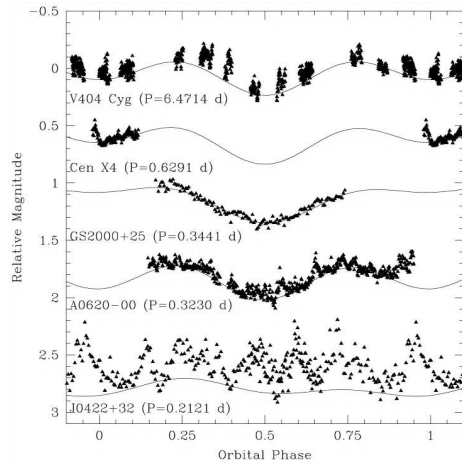


Fig. 5 High-time resolution light curves of quiescent XRTs showing the presence of fast variability. From Zurita et al. (2003).

light curves over many orbital cycles. The aperiodic variability can also vary with time for any particular system as shown by several cases in the literature (e.g. BW Cir: Casares et al. 2009; XTE J1859+226: Corral-Santana et al. 2011).

Using a decade-long data set of multicolour quiescent photometry, Cantrell et al. (2008) identify two main states of variability in A0620-00. The so-called *passive* and *active* states fall in separate parts of a colour-magnitude diagram. The system becomes redder in the *passive* state and displays minimum flaring activity (Fig. 6). Ellipsoidal fits to a subset of *passive* *VIH* light curves separately yield an inclination which is $\sim 10^\circ$ higher than previous works have suggested (Cantrell et al. 2010). The latter were based on pure ellipsoidal fits to NIR light curves where the non-stellar contribution was neglected. Consequently, the mass of the BH in A0620-00 can be overestimated by a factor ≈ 2 if the disc contamination is ignored. This work has demonstrated that it is critical to employ light curves with minimum flickering activity during *passive* states to measure unbiased binary inclinations. Further discussion on the impact of the rapid variability in mass determinations of other BH XRTs is presented in Kreidberg et al. (2012).

One of the peculiar properties of the sample of BH XRTs listed in Table 1 is the absence of binaries with inclinations $i > 75^\circ$. Furthermore, none of the other ~ 33 BH candidates (i.e. those XRTs with similar X-ray properties to dynamical BHs) shows eclipses, whereas ~ 20 percent are expected for a random distribution of inclinations (although this number is dependent on the assumed mass ratio, q). The lack of eclipsing BH XRTs is intriguing and strongly suggests that an observational bias is at play. It has been proposed that high inclination systems are hidden from view due to obscuration of the central X-ray source by a flared accretion disc (Narayan & McClintock 2005). The recent discovery of optical dips in the XRT Swift J1357.2–0933 suggests that the first extreme inclination BH transient may have been detected (Fig. 7). Aside from the unusual optical dips, the system is remarkable because of its extremely broad H_α emission profile and very low peak X-ray luminosity, properties which can be explained by orientation effects in an edge-on geometry (Corral-Santana et al. 2013; but see Armas Padilla 2013a, 2013b for a different interpretation which proposes an intrinsically faint XRT). Based on the double-peak separation and radial velocities of the H_α profile indirect prove for a BH in a 2.8 hr orbit is presented.

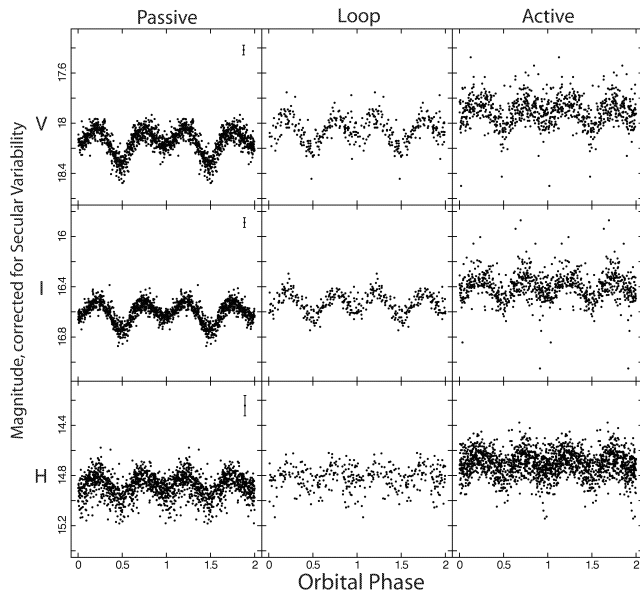


Fig. 6 Ellipsoidal light curves of A0620-00 in three different quiescent states: *passive* (left panels), *loop* (middle panels) and *active* (right). The strength of the aperiodic variability increases from the *passive* to the *active* state. From Cantrell et al. (2008).

In addition, evidence is provided for the presence of an obscuring torus in the inner disc. This brings a new ingredient to theoretical modelling of inner disc flows and jet collimation mechanisms in stellar-mass BHs. The discovery of edge-on BH XRTs is important because these systems will likely deliver the most precise BH mass determinations. Therefore, they will be key in the construction of the mass distribution of compact remnants.

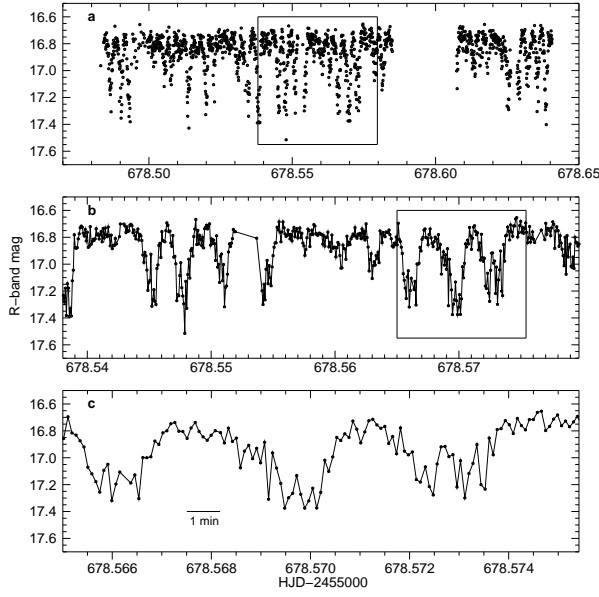


Fig. 7 Optical light curves of Swift J1357.2–0933 during outburst at 7 s time resolution. Regular dips repeating every 2 min cause a drop in brightness of up to $\simeq 0.8$ mag. Close ups with lengths of 1 h and 15 min are displayed in the middle and bottom panels, respectively. From Corral-Santana et al. (2013).

Table 1 Mass measurements of BHs in XRTs (continues on next page). We mark in bold face the measurements we consider the most reliable currently available in the literature.

System	Donor Spect. Type	P_{orb} [days]	$f(M)$ [M_{\odot}]	q	i [deg]	M_{x} [M_{\odot}]	Ref.
GRS 1915+105	K1/5 III	33.5(1.5)	9.5 ± 3.0	0.058 ± 0.033	66 ± 2	14.0 ± 4.4	[1-2]
..		33.8(1)	8.0 ± 0.6		66 ± 2	12.0 ± 1.4	[3]
..		33.85(16)	7.02 ± 0.17	0.042 ± 0.024	66 ± 2	10.1 ± 0.6	[4]
V404 Cyg	K0 IV	6.47129(7)	6.07 ± 0.05	0.067 ± 0.005			[5-7]
..					60–80	8–12	[8]
..					56 ± 4	12_{-2}^{+3}	[9]
..					56 ± 2		[10]
..					> 62	$\lesssim 12.5$	[11]
..	K3 IV				67_{-1}^{+3}	$9.0_{-0.6}^{+0.2}$	[12]
XTE J1819.3-2525	B9 III	2.81730(1)	2.74 ± 0.12	$0.63 - 0.70$	60–71	8.7–11.7	[13]
GRO J1655-40	\sim F5 IV	2.601(27)	3.16 ± 0.15				[14]
..	F3/6 IV	2.62157(15)	3.24 ± 0.09	0.33 ± 0.01	69.5 ± 0.1	7.0 ± 0.2	[15]
..		2.62168(14)		0.24–0.41	63.7–70.7	6.3–7.6	[16]
..		2.62191(20)		0.34–0.4	70.2 ± 1.9	6.3 ± 0.5	[17]
..	F5/G0 IV			0.26 ± 0.04	68.7 ± 1.5	5.4 ± 0.3	[18]
..	F6 IV		2.73 ± 0.09	0.34–0.44		5.5–7.9	[19]
..				0.31 ± 0.08		7.9 ± 3.8	[20]
..				0.42 ± 0.03		6.6 ± 0.5	[21]
..		2.62120(14)	3.16 ± 0.15	0.33 ± 0.05			[22]

System	Donor Spect. Type	P_{orb} [days]	$f(M)$ [M_{\odot}]	q	i [deg]	M_x [M_{\odot}]	Ref.
BW Cir	~G5 IV	2.54451(8)	5.73±0.29	0.12$^{+0.03}_{-0.04}$	<79	>7.0	[23-24]
GX 339-4	–	1.7557(4)	5.8±0.5			>6.0	[25-26]
XTE J1550-564	K2/4 IV	1.5420333(24)	7.65±0.38	≈0.03	74.7±3.8	7.8–15.6	[27-28]
4U 1543-475	A2 V	1.123(8)	0.22±0.02		20–40	2.7–7.5	[29]
H1705-250	K3/M0 V	0.5213(13)	4.86±0.13	≤0.053	60–80	4.9–7.9	[30-32]
„					48–51		[33]
GS 1124-684	K3/5 V	0.4326058(31)	3.01±0.15	0.13±0.04			[34-36]
„					60 $^{+5}_{-6}$	5.0–7.5	[36]
„					54 $^{+20}_{-15}$	5.8 $^{+4.7}_{-2.0}$	[37]
„					54±2	7.0±0.6	[38]
GS 2000+250	K3/7 V	0.3440915(9)	5.01±0.15	0.042±0.012			[39-41]
„					65±9	8.5±1.5	[42]
„					43–69	4.8–14	[43]
„		0.3440873(2)			58–74	5.5–8.8	[44]
A0620-00	K2/7 V	0.323014(1)	2.91±0.08		<50	>7.3	[45-46]
„			2.72±0.06	0.067±0.010			[47]
„			2.76±0.04	0.060±0.004			[48]
„		0.32301405(1)	2.76±0.01				[49]
„					63–74	4.1–5.4	[50]
„					31–54	10 $^{+7}_{-5}$	[51]
„	K3/7 V				38–75	3.3–13.6	[52]
„					41±3	11.0±1.9	[53]
„					51±0.9	6.6±0.3	[54]
XTE J1650-500	≈K4 V	0.3205(7)	2.73±0.56		>47		[55]
GRS 1009-45	K7/M0 V	0.285206(14)	3.17±0.12				[56]
„					37–80		[57]
XTE J1859+226	≈K5 V	0.274(2)	4.5±0.6		<70	> 5.42	[58-59]
GRO J0422+32	M0/4 V	0.21159(57)	1.21±0.06	0.12 $^{+0.08}_{-0.07}$			[60-63]
„	M4/5 V	0.2121600(2)	1.19±0.02	0.11$^{+0.05}_{-0.02}$	<45	>2.2	[64]
„	M0/4 V				35–49	~2.5–5.0	[61]
„					≤45		[65]
„					10–26	≥15	[66]
„					45±2	3.97±0.95	[67]
„				< 0.04	<30	≥10.4	[68]
XTE J1118+480	K5/M1 V	0.1699339(2)	6.27±0.04	0.024±0.009			[69-73]
„				0.037±0.007			[74]
„					68±2	8.30 $^{+0.28}_{-0.14}$	[75]
„	K7/M1 V				68–79	6.9–8.2	[76]

REF: [1] Greiner et al. (2001); [2] Harlaftis & Greiner (2004); [3] Hurley et al. (2013); [4] Steeghs et al. (2013); [5] Casares et al. (1992); [6] Casares & Charles (1994); [7] Casares (1996); [8] Wagner et al. (1992); [9] Shahbaz et al. (1994b); [10] Pavlenko et al. (1996); [11] Sanwal et al. (1996); [12] Khargharia et al. (2010); [13] Orosz et al. (2001); [14] Bailyn et al. (1995); [15] Orosz & Bailyn (1997); [16] van der Hooft et al. (1998); [17] Greene et al. (2001); [18] Beer & Podsiadlowsky (2002); [19] Shahbaz et al. (1999); [20] Buxton & Vennes (1999); [21] Shahbaz (2003); [22] González Hernández et al. (2008b); [23] Casares et al. (2004); [24] Casares et al. (2009); [25] Hynes et al. (2003a); [26] Muñoz-Darias et al. (2008a); [27] Orosz et al. (2002); [28] Orosz et al. (2011a); [29] Orosz et al. (1998); [30] Remillard et al. (1996); [31] Filippenko et al. (1997); [32] Harlaftis et al. (1997); [33] Martin et al. (1995); [34] Remillard et al. (1992); [35] Casares et al. (1997); [36] Orosz et al.

(1996); [37] Shahbaz et al. (1997); [38] Gelino et al. (2001a); [39] Casares et al. (1995b); [40] Filippenko et al. (1995b); [41] Harlaftis et al. (1996); [42] Callanan et al. (1996b); [43] Beekman et al. (1996); [44] Ioannou et al. (2004); [45] McClintock & Remillard (1986); [46] Orosz et al. (1994); [47] Marsh, Robinson & Wood (1994); [48] Neilsen et al. (2008); [49] González Hernández & Casares (2010); [50] Haswell et al. (1993); [51] Shahbaz et al. (1994a); [52] Froning & Robinson (2001); [53] Gelino et al. (2001b); [54] Cantrell et al. (2010); [55] Orosz et al. (2004); [56] Filippenko et al. (1999); [57] Shahbaz et al. (1996); [58] Filippenko & Chornock (2001); [59] Corral-Santana et al. (2011); [60] Orosz & Bailyn (1995); [61] Casares et al. (1995a); [62] Filippenko et al. (1995a); [63] Harlaftis et al. (1999); [64] Webb et al. (2000); [65] Callanan et al. (1996a); [66] Beekman et al. (1997); [67] Gelino & Harrison (2003); [68] Reynolds et al. (2007); [69] Wagner et al. (2001); [70] McClintock et al. (2001); [71] Torres et al. (2004); [72] González Hernández et al. (2008a); [73] Calvelo et al. (2009); [74] Orosz et al. (2001); [75] Gelino et al. (2006); [76] Khargharia et al. (2013)

NOTES TO TABLE 1: **GRS 1915+105**: the inclination angle is derived from the orientation of radio jets (Fender et al. 1999). Note that the radial velocity curve, and thus the BH mass, might be affected by irradiation because the binary has remained active since its discovery, although there are currently no signs for such effects.

V404 Cyg: [10] model the lower envelope of an I-band light curve to minimize flickering contribution, but do not account for dilution from non-variable disc light. Optical spectroscopy indicates veiling is very small at RI wavelengths but the impact in ellipsoidal modeling should be tested through simultaneous photometric and spectroscopic observations. [9] model a K-band light curve assuming no disc contribution while [11] demonstrate significant flickering is present in the H-band. [12] fit the H-band light curve of [11] after correcting for the disc contribution which is, however, estimated from non-simultaneous NIR spectroscopy.

XTE J1819.3-2525: limits to the inclination angle are derived from ellipsoidal fits to a low quality archival photographic light curve.

GR0 J1655-40: the mass functions reported in [14-15] are likely biased by irradiation effects. [19] and [22] quote mass functions in true quiescence but they disagree at $> 3\sigma$ level. The latter is obtained from an orbital solution with sparse phase coverage, resulting in a significantly different period and systemic velocity with respect to previous studies. Therefore, we tentatively favour the former solution although this issue needs to be investigated further. [15-18] report q values derived from fits to the ellipsoidal modulations, the others are obtained from $V \sin i$. [21] determine q by fitting line profiles with synthetic spectra computed using NEXTGEN model atmospheres in a Roche geometry, accounting for variations in temperature and gravity. We favour this q determination. [18] fit BVRI light curves from [15] simultaneously, using Kurucz model atmospheres. The distance and colour excess are not fixed but included in the fit as free parameters, and the best (adopted) solution assumes the distance from Hjellming & Ruppen (1995). We tentatively favour the inclination reported in [18] although it should be noted that the q value implied by their ellipsoidal fits is significantly lower than our favoured value. In any event, there is an excellent agreement between all inclination values reported by four different groups. This is the only case where the error on the BH mass is dominated by uncertainties in q and the mass function rather than in the inclination. We tentatively favour the BH mass reported in [21] because it is based on both our favoured q and mass function from [19], which is free from irradiation effects. The BH mass quoted in the abstract of [21] is wrong due to a typo (Shahbaz, private communication).

BW Cir: the light curves are dominated by strong flickering which disguises the ellipsoidal modulation.

GX 339-4: the mass function is based on radial velocities of Bowen emission lines emanating on the inner hemisphere of the irradiated donor.

XTE J1550-564: [28] derive inclination constraints by simultaneously fitting optical and NIR lightcurves. Conservative BH masses are quoted after allowing for different values of disc contribution obtained through non-simultaneous spectroscopy.

4U 1543-475: low inclinations are implied by the small amplitude of some low quality VI-band ellipsoidal light curves. However, quoted values should be treated with caution because of possible systematics derived from model assumptions, namely disc light is neglected and the early type donor is assumed to be synchronized and filling its Roche lobe.

H1705-250: the limited spectral resolution in the spectra reported in [32] only allow one to set an upper limit

to q . [30] derive broad limits to the inclination based on the absence of eclipses ($i < 80^\circ$) and assuming no disc contribution in a V-band lightcurve ($i > 60^\circ$).

GS 1124-684: [37-38] derive inclinations assuming no disc contribution to the NIR light curves. The latter authors also quote uncertainties which seem unrealistically small given potential systematic effects. While [36] tries to account for disc veiling in their B+V & I-band lightcurves, large deviations from ellipsoidal morphology make the derived inclinations suspect. Note also that this XRT is strongly affected by large amplitude flickering (Hynes et al. 2003b; Shahbaz et al. 2010).

GS 2000+250: the mass ratio reported in [41] should be treated with some caution because of the limited spectral resolution of the spectroscopic observations. [42-43] neglect any disc contribution in their ellipsoidal fits to NIR light curves. Inclinations reported in [44] are tentatively favoured because modeling accounts for a hot-spot component and the maximum disc light contribution (<32 percent in the R-band) allowed by the absence of X-ray eclipses.

A0620-00: the q value reported in [47] is slightly preferred over that in [48] because the former accounts for the non-sphericity of the Roche lobe, although this correction may not be statistically significant. In any case both determinations are fully consistent.

GRS 1009-45: wide limits to the inclination are obtained from the absence of X-ray eclipses and ellipsoidal fits to an R-band light curve, assuming no disc contribution.

XTE J1859+226: light curves are dominated by strong episodic flickering.

GR0 J0422+32: the reported mass ratios should be treated with some caution because of the limited spectral resolution of the spectroscopic data. All inclinations reported are suspected because of very large flickering amplitude in optical and NIR light curves.

XTE J1118+480: the q value reported in [73] has been corrected for orbital smearing of the line due to the motion of the mass donor during the exposure. Inclination and BH masses given in [76] are slightly preferred over those in [75] because the latter are based on multiwavelength ellipsoidal fits to BVRJHK lightcurves which are non-simultaneous. [76] only fits H-band light curves but the disc contribution is accounted for via contemporaneous NIR spectroscopy. It also provides a wider range of inclinations which is seen as more realistic. A period derivative for the orbital period of $\dot{P} = -1.83 \pm 0.66 \text{ ms yr}^{-1}$ was derived by González Hernández et al. (2012).

3 Dynamical Black Holes in High-Mass X-ray Binaries (HMXBs)

In addition to the 17 transients listed in Table 1, dynamical mass measurements of BHs have also been possible for four X-ray binaries with high-mass donor stars: Cyg X-1 and the extragalactic sources LMC X-1, LMC X-3 and M33 X-7. HMXBs are persistent X-ray sources, with typical X-ray luminosities $\sim 10^{37} \text{ ergs s}^{-1}$ powered by massive stellar winds or incipient Roche lobe overflow. Despite being persistent X-ray sources, irradiation effects are mostly negligible because the X-ray luminosity is smaller than or comparable to the bolometric luminosity of the mass-losing star. Further, the contribution of the accretion disc to the total optical flux can be ignored and thus ellipsoidal light curves are not affected by systematic effects as discussed in the previous section. There are, however, two important limitations regarding mass determination in HMXBs. First, the BH mass is very sensitive to uncertainties in the mass of the optical star. The latter is highly uncertain because donor stars in HMXBs are typically undermassive for their spectral types due to secular mass transfer and binary evolution (Rappaport & Joss 1983; Podsiadlowski et al. 2003; also compare spectral types and donor masses implied by Table 2). Second, mass transfer in HMXBs is mostly powered by stellar winds rather than Roche lobe overflow and this has a two-fold effect. On the one hand, wind emission can contaminate radial velocities from the massive

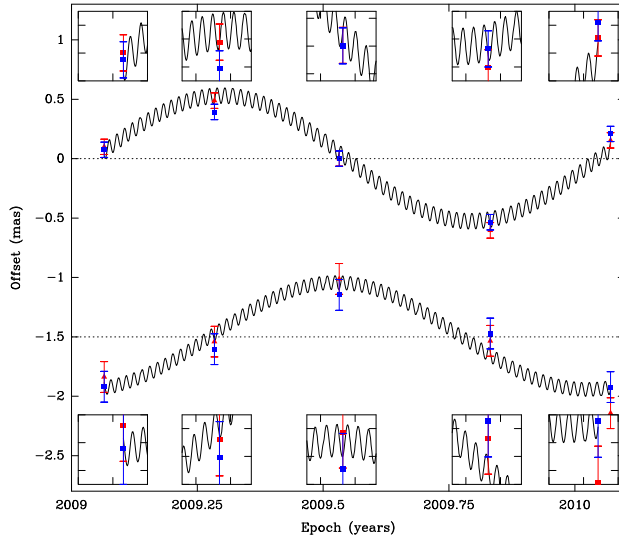


Fig. 8 Astrometric parallax of the compact radio source in Cyg X-1. The long sinusoid indicates the annual parallax after removing the proper motion of the system. The short period sinusoid reflects the 5.6 day orbit of the BH around the center of mass of the binary. From Reid et al. (2011).

star, specially if these are obtained from lower excitation Balmer lines (e.g. Ninkov et al. 1987). On the other hand, if the companion star is not filling its Roche lobe then one of the previous assumptions breaks down and q and i can be underestimated if derived from $V \sin i$ and ellipsoidal models as before. To circumvent this problem, extra parameters need to be included when modeling the observations, namely the Roche lobe filling factor and the degree of synchronization of the companion star (e.g. Gies & Bolton 1986; Orosz et al. 2007).

Despite these caveats, accurate masses can still be obtained if dynamical constraints are combined with a determination of the radius of the optical star. Accurate knowledge of the luminosity and hence the distance is required which is often difficult. For example, BH masses reported for Cyg X-1 over the last 3 decades show a large dispersion, with values between $7\text{-}29 M_{\odot}$, mainly owing to distance uncertainties. Fortunately, a major advance has been allowed by the determination of the trigonometric parallax distance of Cyg X-1 with VLBA. Reid et al. (2011) have used emission from the compact radio jet to trace the position of the BH over 1 year. A parallax of $0.539 \pm 0.033 \text{ mas}$ has been derived which in turn implies a distance of $1.86 \pm 0.12 \text{ kpc}$. The astrometric measurements are even sensitive to the size of the BH orbit allowing to constrain its radius to $0.18 \pm 0.09 \text{ AU}$ (Fig. 8). Using the accurate distance as an extra constraint to the dynamical model, a BH mass of $14.8 \pm 1.0 M_{\odot}$ is derived, one of the most precise determinations to date (Orosz et al. 2011b). The best model solution also proves that the binary orbit is slightly eccentric ($e \simeq 0.02$) and the companion star rotates faster than the synchronization value at periastron.

Another remarkable result has been reported for M33 X-7, the first eclipsing stellar-mass BH. M33 X-7 is located in the nearby spiral galaxy M33 and hosts a late O companion which eclipses the X-ray source every 3.45 days (Larson & Schulman 1997). Ellipsoidal fits to the optical light curves alone have suggested the presence of a BH companion (Pietsch et al. 2006) but confirmation through radial velocities became challenging because of crowding

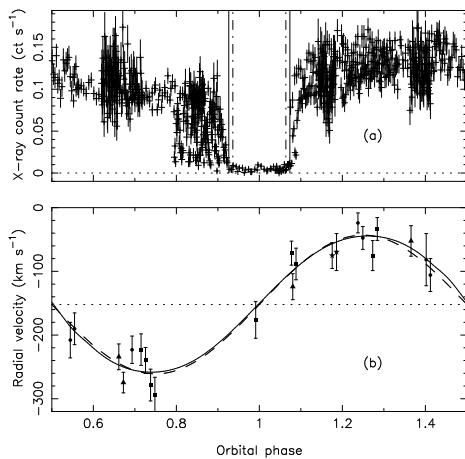


Fig. 9 (a) Chandra X-ray light curve of M33 X-7 showing the eclipse of the compact source by the optical companion. (b) Radial velocity curve of the O7-8III companion star. From Orosz et al. (2007).

and contamination by nebular lines. A radial velocity curve of the O7-8III companion was finally reported in Orosz et al. (2007), together with updated ellipsoidal fits (Fig. 9). The duration of the eclipse and the distance to M33 provides new restrictions which tightly constrain the parameter space of the dynamical model, in particular the binary inclination, the companion radius and its filling factor. As in Cyg X-1, the orbit is found to be slightly eccentric, while the radius of the donor star extends up to 78 percent of its Roche lobe. The best fit yields a BH mass of $15.7 \pm 1.5 M_{\odot}$, one of the largest accurately known. The companion star is underluminous for its spectral type and, with $70.0 \pm 6.9 M_{\odot}$, it is also one of the most massive stars known with high accuracy. M33 X-7 strongly impacts theories of BH formation and binary evolution since it is very hard to produce this massive HMXB in such a tight orbit (Valsecchi et al. 2010).

Table 2 lists a summary of fundamental parameters in the four HMXBs with dynamical BH mass measurements. In some cases, early mass estimates were derived after assuming that the optical star is synchronized and/or filling its Roche lobe. However, the most accurate results were subsequently obtained through fitting the ensemble of light curves, radial velocities and projected rotational velocities with a full model parametrization. These models account for non-synchronous rotation, Roche lobe filling fraction and (sometimes) eccentricity. As mentioned above, a determination of the distance, which is constrained to better than 6 percent in the four HMXBs, is key to deliver accurate BH masses. Despite this, a precise BH mass for LMC X-3 is not yet available because of the large impact of X-ray heating in the analysis. Note that we only quoted BH masses derived using the dynamical mass measurement method explained above. Mass estimates based on other techniques, such as fitting model atmospheres (Herrero et al. 1995; Caballero-Nieves et al. 2009), stellar evolutionary models (Ziółkowski 2005) or scaling X-ray spectral/timing properties (Shaposhnikov & Titarchuk 2007), are not considered here. Albeit with low number statistics, Table 2 shows that BHs in HMXBs have typically a mass $>10 M_{\odot}$ and hence they tend to be more massive than BHs in XRTs. This seems to hint at an evolutionary difference, with BHs in HMXBs descending from massive progenitors which may have experienced comparatively lower stellar wind mass-loss rates, possibly through case C mass transfer (Wellstein & Langer 1999). Low metallicity environments, which strongly influence

Wolf-Rayet mass-loss rates and the radius evolution of progenitor stars, is another important factor in the three extragalactic HMXBs (Crowther et al. 2010). It has also been proposed that BHs more massive than $\sim 10 M_{\odot}$ may form through direct implosion of the core remnant (Mirabel & Rodrigues 2003) although it remains unclear why prompt collapse should have a larger incidence in HMXBs.

We did not include the mass measurements for the two extra-Galactic HMXBs NGC 300 X-1 and IC 10 X-1 by Crowther et al. (2010) and Silverman & Filippenko (2008), respectively, as we deem these mass measurements less secure than those of the four sources we list in Table 2. The main reason for this is that the BH mass is strongly dependent on the assumed mass of the Wolf-Rayet star. The latter depends on the assumed stellar luminosity of the Wolf-Rayet star which in turn can be influenced by contamination from unresolved stars in the galaxies under study. These two sources are nevertheless very interesting as they may harbor BHs with the largest masses measured so far.

Several authors have examined the mass distribution of stellar mass BHs in order to gain insight into BH formation models. Bayesian analysis of the observed distribution suggests the presence of a mass gap or dearth of compact objects in the interval $\sim 2-5 M_{\odot}$ (Özel et al. 2010; Farr et al. 2011). This has been interpreted in the context of supernova models by a rapidly evolving explosion (within 0.2 s after the core bounce) through a Rayleigh-Taylor instability (Belczynski et al. 2012). On the other hand, the absence of low mass BHs has been attributed to a potential observational artefact caused by the systematic uncertainties affecting ellipsoidal fits and hence inclination measurements (see Section 2.1; Kreidberg et al. 2012). This has a strong impact on BH formation scenarios since confirmation of a mass gap would rule out accretion induced collapse while it would support delayed supernova explosion models. Future accurate mass measurements of BHs in high-inclination systems will allow testing whether the mass gap is caused by systematics in the binary inclination or it is a signature of the BH formation mechanism. This involves discovering new favourable XRTs and also exploiting novel techniques for mass measurements.

4 Future perspectives

The best prospects to enlarge the current sample of stellar-mass BHs are offered by new discoveries of XRTs. Figure 10 presents the cumulative number of BH XRTs discovered in the X-ray astronomy era, starting with the historic detection of Cen X-2 by a rocket flight in 1966. A linear increase is apparent since the late 80's, when X-ray satellites with increased sensitivity and All-Sky-Monitors became operational. This sets a discovery rate of ~ 1.7 XRTs yr^{-1} . Extrapolation of the number of XRTs detected to date suggests that several thousand “dormant” BHs remain to be discovered (Romani 1998). And this estimate is most likely biased low because of sample incompleteness and complex selection effects. In particular a likely population of long period XRTs with very long outburst duty cycles is often ignored (c.f. Ritter & King 2002). In addition, there is mounting evidence for the existence of a significant number of intrinsically faint or obscured XRTs (Degenaar & Wijnands 2010; Corral-Santana et al. 2013). Incidentally, the latest population-synthesis models predict $\sim 10^3 - 10^4$ XRTs in the Galaxy (Yungelson et al. 2006; Kiel & Hurley 2006). In either case, the observed sample is just the tip of the iceberg of a large “hibernating” population which becomes slowly unveiled through outburst episodes (van den Heuvel 1992). Figure 10 also shows that only 17 BH XRTs have been dynamically confirmed, representing about 30 percent of the total number discovered. The remaining ones are virtually lost during decay to quiescence because they become too faint, even for 10m-class telescopes. Therefore,

Table 2 Mass measurements of BH in HMXBs. We mark in bold face the measurements we consider the most reliable currently available in the literature.

System	Donor Spect. Type	P_{orb} [days]	$f(M)$ [M_{\odot}]	q	i [deg]	M_x [M_{\odot}]	Ref.
Cyg X-1	~B0Ib	~5.607	~0.16			>3	[1-2]
..	09.7 Iab	5.5995(9)	0.182	≈ 2.1	≈ 30	≈ 14	[3]
..		5.59974(8)	0.25 ± 0.01	1.95–2.31	28–38	16 ± 5	[4-5]
..		5.599829(16)	0.244 ± 0.006	1.29 ± 0.15	27.1 ± 0.8	14.8 ± 1.0	[6]
LMC X-1	07 III	4.2288(6)	0.14 ± 0.05	$\gtrsim 2$	40–63	≈ 6	[7-8]
..		3.90917(5)	0.149 ± 0.007	4.91 ± 0.53	36.4 ± 1.9	10.9 ± 1.4	[9]
M33 X-7	07-8 III	3.453014(20)	0.46 ± 0.08	4.47 ± 0.60	74.6 ± 1.0	15.7 ± 1.5	[10]
LMC X-3	B3 V	1.70491(7)	2.3 ± 0.3		50–70	7–14	[11]
..	B3-5V	1.70479(4)	2.99 ± 0.17		50–70	9.5–13.6	[12]
..		1.7048089(11)	2.77 ± 0.04				[13]

REF: [1] Webster & Murdin (1972); [2] Bolton (1972a); [3] Bolton (1972b); [4] Gies & Bolton (1982); [5] Gies & Bolton (1986); [6] Orosz et al. (2011b); [7] Hutchings et al. (1983); [8] Hutchings et al. (1987); [9] Orosz et al. (2009); [10] Orosz et al. (2007); [11] Cowley et al. (1983); [12] Val-Baker et al. (2007); [13] Song et al. (2010)

NOTES TO TABLE 2: **Cyg X-1:** [3] uses ellipsoidal light curves from Cherepashchuk et al. (1973) to constrain q and i , assuming the star fills the Roche lobe. Also assumes a $30 M_{\odot}$ companion to estimate the BH mass. [5] assumes synchronization and fill-out factor in the range 0.9–1. [6] uses the orbital period determination, radial velocity data and light curves from Brocksopp et al. (1999). Also adopts a rotational broadening determination from Caballero-Nieves et al. (2009).

LMC X-1: [7-8] use a lower limit to q from radial velocities of the NIII $\lambda 4640$ emission. Synchronization is also assumed to derive a lower limit to the inclination.

M33 X-7: [10] adopts the orbital period determination from X-ray eclipses (Pietsch et al. 2006).

LMC X-3: [11] assumes synchronization to derive a lower limit to the inclination. [12] finds evidence of irradiation in the donor star and the BH mass has been corrected for it.

improving on the statistics of BH masses requires not only a new generation of ELT telescopes to tackle fainter targets but also new strategies aimed at unveiling a large fraction of the “hibernating” population of quiescent XRTs. A promising approach is presented by the *Galactic Bulge Survey* (GBS), where potential quiescent BH XRTs are selected in Chandra observations of regions in the Galactic Bulge 1 degree away from the Galactic plane (Jonker et al. 2011; Torres et al. 2013).

4.1 Reprocessed Bowen emission

New opportunities for the study of BH XRTs are also opened by the analysis of emission lines and timing properties of the X-ray reprocessed radiation. To start with, the discovery of sharp high-excitation emission lines in active X-ray binaries have demonstrated that dynamical information can also be extracted from XRTs while in outburst (Steeghs & Casares 2002). These lines, first detected in the neutron star binary Sco X-1, arise from reprocessing in the irradiated companion. The most prominent are the NIII $\lambda 4634$ -40 and CIII $\lambda 4647$ -50 triplets in the core of the Bowen blend (Fig. 11). In particular, the NIII lines are powered by fluorescence resonance which requires seed photons of HeII Ly α . Since the velocities of the Bowen lines trace the orbit of the illuminated hemisphere, a K-correction (which chiefly

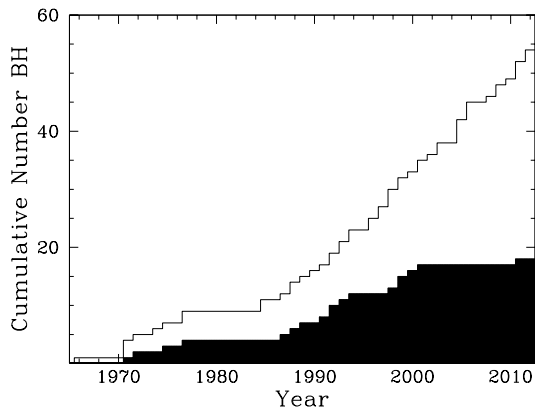


Fig. 10 Cumulative distribution of BH XRTs discovered during the era of X-ray astronomy. The black histogram indicates XRTs with BHs proven dynamically. Note, however, that the black histogram indicates the times when dynamical BHs were first discovered by X-ray satellites and not when the actual mass functions were measured/reported. The latest dynamical mass measurement BH corresponds to Swift J1357.2-0933 although the evidence is indirect (see Corral-Santana et al. 2013). Updated after Casares (2010).

depends on the mass ratio and the disc flaring angle) needs to be applied in order to obtain the true radial velocity curve of the donor star center of mass (Muñoz-Darias et al. 2005). The discovery of sharp Bowen lines during the 2002 outburst of GX 339-4 has allowed the first determination of the mass function in this Rosetta stone XRT and therefore the dynamical proof of a BH (Hynes et al. 2003a; Muñoz-Darias et al. 2008a; see Fig. 11). This work illustrates the power of the technique for systems which otherwise cannot be studied in quiescence because they become too faint for current instrumentation.

Second, the timing properties of the reprocessed light allows one to perform Echo Tomography experiments. Echo Tomography exploits time delays between X-ray and UV/optical variability as a function of orbital phase to map the illuminated sites in a binary (O’Brien et al. 2002). In particular, radiation reprocessed in the companion star gives rise to a sinusoidal modulation of time lag versus orbital phase. The shape of the modulation encodes information on the most fundamental parameters such as the binary inclination, mass ratio and stellar separation. Therefore, Echo Tomography offers an alternative route to derive accurate inclinations, which is critical for measuring BH masses. Unfortunately, attempts to measure correlated optical/X-ray variability using broad-band filters have resulted in little evidence for orbital modulation, with time lags pointing to reprocessing in the outer disc (Hynes 2005). Alternatively, the use of emission line light curves allows one to amplify the response of the donor’s contribution by suppressing most of the background continuum light, dominated by the disc. This requires special instrumentation such as *ULTRACAM* (Dhillon et al. 2007), a high-speed triple-beam CCD camera, equipped with customized narrow-band filters centered in the Bowen blend and a nearby continuum. Following this strategy, time lags associated with the donor star have been finally presented for the neutron star X-ray binaries Sco X-1 and 4U 1636-536 (Muñoz-Darias et al. 2007, 2008b). In the latter case, three X-ray/optical bursts were observed at different orbital phases and their time lags were found to be consistent with those simulated for a plausible range of binary masses and inclinations. A careful subtraction of the underlying continuum seems critical to deliver unbiased incli-

nations and this requires further investigation. Echo Tomography has not been attempted on BH XRTs yet because it is very difficult to coordinate space facilities with adequate ground-based instruments, such as *ULTRACAM*, in ToO mode. The most efficient use of the technique would require implementing a fast read-out optical/UV camera onboard of an X-ray satellite. The camera should be provided with frame transfer EM3CCDs and a dual-channel, optimized for the Bowen lines (either in the optical or the higher energy OIII $\lambda 3133/\lambda 3444$ transitions) and an adjacent continuum. Such an instrument would guarantee both simultaneity and an optimal continuum subtraction.

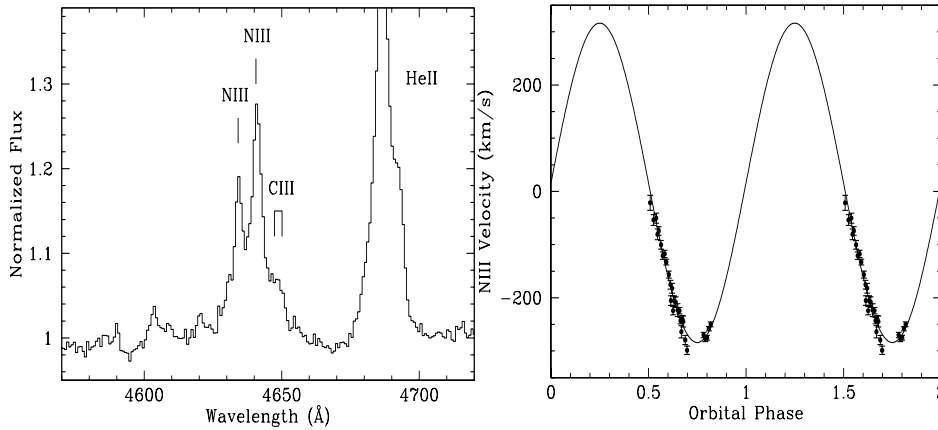


Fig. 11 Detecting companion stars in persistent X-ray binaries and XRTs in outburst. Left: high excitation emission lines from the irradiated donor in GX 339-4. Right: radial velocity motion of the Bowen CIII/NIII emission lines in GX 339-4 as a function of time. Adapted from Hynes et al. (2003a).

4.2 Optical/NIR Interferometry

A different avenue to obtain accurate inclinations relies on measuring the astrometric orbits of the companion stars to the BHs. Table 3 lists the angular size (a/d) of the companion's orbits for the best candidates, with values ranging between 20-60 μas . Resolving the projected orbits thus requires astrometry at micro-arcsec level which is technically challenging. Fortunately, prospects are bright thanks to new developments on optical/NIR interferometry in ground-based and space instrumentation. Three main facilities will be capable of measuring the orbits of some of the targets listed in Table 3: *GRAVITY*, *GAIA* and the proposed *Space Interferometry Mission SIM Lite* (Unwin et al. 2008). *GRAVITY*, a second generation instrument on VLTI, is scheduled to see first light in 2014 (Kendrew et al. 2012). With a goal of 10 μas precision astrometry for targets brighter than $K=15$ it can potentially resolve the companion's orbit in GRS 1915+105. V404 Cyg and Cyg X-1 are also within reach,

Table 3 Best BH candidates for astrometric orbit determination

System	P_{orb} [days]	d [kpc]	a/d [μas]	V mag	K mag
V404 Cyg	6.5	2.4	61	18.4	12.4
Cyg X-1	5.6	1.9	45	8.9	6.5
GRS 1915+105	33.5	11.5	40	>25	13.0
A0620-00	0.33	1.1	20	18.3	14.5
GRO J1655-40	2.6	3.2	18	17.2	13.2

although pushing the observations to high airmasses. On the other hand, *SIM Lite* is designed to deliver micro-arcsecond astrometry in the optical band down to $V = 19$. While Cyg X-1 can be easily tackled, V404 Cyg is at the limit because of its optical faintness. Finally, *GAIA* will allow to measure the orbital motion of the companion star in Cyg X-1. The first direct measurements of binary orbits will clearly represent a major step forward in the knowledge of the fundamental parameters of these systems. Not only BH masses could be determined to better than 10 percent accuracy, but also precise inclinations for a sample of BHs will allow to quantify the impact of systematic errors in ellipsoidal light curve modeling. In addition, interferometry will deliver accurate distances and proper motions, key quantities to determine the BH natal kick and thus constrain the formation and evolution history of accreting BH X-ray binaries (e.g. Wong et al. 2012). Currently, parallax distances are only available for Cyg X-1 (Lestrade et al. 1999; Reid et al. 2011) and V404 Cyg (Miller-Jones et al. 2009) through radio Very Long Baseline Interferometry observations. The advent of the optical/NIR interferometry era will allow one to extend these measurements to any (sufficiently bright) BH binary in the Galaxy.

5 Intermediate-mass black holes?

As one has seen above, stellar black holes with masses up to $\sim 16M_{\odot}$ (see Table 1 and 2) have been found. Theoretically, the mass of a stellar mass black hole depends on the initial mass of the progenitor, how much mass is lost during the progenitor’s evolution and on the supernova explosion mechanism (Belczynski et al. 2010; Fryer et al. 2012). Mass is lost through stellar winds, the amount of mass lost strongly depends on the metallicity of the star. For a low-metallicity star (~ 0.01 of the solar metallicity) it is possible to leave a black hole of $\lesssim 100 M_{\odot}$ (Belczynski et al. 2010).

Thus, these models do allow for more massive stellar-mass black holes than have been found so far in our Galaxy. In current stellar evolution models the mass distribution of black hole remnants from massive stars peaks around $10 M_{\odot}$, with a tail up to the said $\lesssim 100 M_{\odot}$. In very massive stars ($\gtrsim 130M_{\odot}$) the production of free electrons and positrons, due to the increased gamma ray radiation, reduces the thermal pressure inside the core. This eventually leads to a runaway thermonuclear explosion that completely disrupts the star without leaving a black hole, causing the upper limit for a stellar black hole of $\sim 100 M_{\odot}$.

Supermassive black holes (SMBHs) in AGN with masses of $> 10^5 M_{\odot}$ (Greene & Ho 2007) have been identified. However, black holes with masses of several hundred to a few thousand solar masses remain elusive. Such intermediate-mass black holes (IMBHs) may be remnants from the first population of zero-metallicity massive stars. These Population III stars could have had masses above the pair-instability limit of around $130 M_{\odot}$ and they may

have collapsed into IMBHs (Madau & Rees 2001). It has also been suggested that IMBHs may form in the centers of dense stellar clusters via the merging of stellar-mass black holes (e.g., Miller & Hamilton 2002), or from the collapse of merged supermassive stars in very dense star clusters (e.g., Portegies Zwart and McMillan 2002). Primordial formation of a population of IMBHs is not ruled out (Afshordi, McDonald and Spergel 2003), although they do not form a significant fraction of the dark matter (Ricotti, Ostriker & Mack 2003).

IMBHs could allow for the assembly of supermassive black holes early in the Universe (e.g. Volonteri 2010; Volonteri 2012). IMBHs may contain a similar or even a larger fraction of the baryonic matter than SMBH and they are potential sources of gravitational waves when they spiral into SMBHs (Madau & Rees 2001). Those IMBHs that were produced early in the life of the Universe but that did not evolve into SMBHs should still be wandering in the (outer) halos of galaxies, such as our Milky way (O’Leary and Loeb 2012; Rashkov and Madau 2013).

So, there is significant interest in finding these IMBHs and observationally determine their properties. A comprehensive review of constraints on the existence of IMBHs can be found in van der Marel (2003). The main problem in finding definitive proof for the existence of IMBHs is that the radius of their sphere of influence is small ($r_{infl} = \frac{GM_{BH}}{v^2}$). The meaning of v depends on the case under consideration: v can be the velocity of a recoiling BH with respect to that of surrounding stars, or for BHs in the centre of a stellar association/cluster it is the velocity dispersion of the stars). Below, we will revisit the possible observational evidence for the existence of IMBHs.

5.1 IMBHs in globular clusters?

Given that several formation mechanisms for IMBHs seem to require dense stellar environments (Miller & Hamilton 2002; Portegies Zwart and McMillan 2002), much effort has gone into investigating whether IMBHs are present in the cores of globular clusters.

5.1.1 Photometric and kinematic evidence

The number of stars as a function of distance (R) to the centre of a globular cluster has been used to investigate whether a central BH is present or not: this function has the form of $N(R) \propto R^{-0.75}$ (Bahcall and Wolf 1976; Bahcall and Wolf 1977). However, a globular cluster that has gone through core collapse (Djorgovski and King 1986) will show a similar distribution of the number of stars as a function of radius from the centre of the globular cluster (e.g. the case of M 15 see Grabhorn et al. 1992).

Instead, using both spectroscopic as well as photometric data and comparing that to a model of stellar orbits in the globular cluster potential one can derive whether a central IMBH is present or not. The observed surface brightness profile together with an assumed mass-to-light ratio and a central IMBH of a given mass provides a model for the kinematics of the stars. This model is compared with the actual kinematics data such as the radial velocity profile and the velocity dispersion as a function of the distance to the cluster centre. The data is fit for the mass-to-light ratio and the mass of the IMBH in the cluster core (which can be zero). IMBHs, if present in the centre of a globular cluster, will increase the velocity dispersion in the core. This method has been used to argue for the presence of IMBHs in a sample of globular clusters (most notably G1 near M 31; Gebhardt et al. 2002; Gebhardt et al. 2005). The presence of compact objects (white dwarfs, neutron stars and stellar-mass BHs that sink to the centre of the cluster due to dynamical friction) does not

significantly alter the conclusion about the presence of an IMBH in the centre of the cluster (Gebhardt et al. 2005). However, conflicting reports on modeling the observable data exist: Baumgardt et al. (2003) obtain good fits to the spectroscopic and the photometric data using N-body calculations without the need of an IMBH (although the work of Gebhardt et al. 2005 challenges this). Lützendorf et al. (2013) compile the globular clusters for which evidence exists that they harbor IMBHs and they further show that these IMBHs do not follow the $M-\sigma$ correlation as found to SMBHs (Ferrarese and Merritt 2000).

5.1.2 Radio – X-ray correlation

For G1, besides the dynamical evidence for the presence of an IMBH, Pooley and Rappaport (2006) showed that there was X-ray emission of a source associated with the globular cluster, however, the spatial scale of their *XMM-Newton* observation did not allow the authors to claim that the source resides in the core of G1. The source luminosity is both consistent with that expected for an IMBH accreting at a low (Bondi-Hoyle) rate as well as with the source being a low-mass X-ray binary (LMXB) accreting via Roche lobe overflow from a companion star. Kong et al. (2010) improved the X-ray position of the source using a *Chandra* observation. The source position is consistent with being equal to the centre of the globular cluster.

Ulvestad et al. (2007) provided evidence for the detection of radio emission from the same location as the X-ray emission. Given that the relation between BH mass, X-ray and radio luminosity appears to follow a fundamental plane, in which the ratio of radio to X-ray luminosity increases as the 0.8 power of the BH mass, an IMBH is more radio loud at a given X-ray luminosity than a stellar-mass BH (Merloni et al. 2003; Falcke et al. 2004). The result of Ulvestad et al. (2007) is consistent with an IMBH scenario but not with an LMXB scenario. However, the radio and X-ray observations were not simultaneous and the significance of the radio detection warranted further investigation. Miller-Jones et al. (2012) conducted the experiment where simultaneous X-ray (*Chandra*) and radio (VLA) observations of G1 were obtained. Whereas the X-ray luminosity was consistent with that found before, these authors find no evidence for radio emission at the position of the X-ray source down to a limit of $4.7 \mu\text{Jy}$ per beam. Using the fundamental plane of BH activity this yields an upper limit on the mass of the IMBH in G1 of $< 9.7 \times 10^3 M_{\odot}$. Note that this upper limit is only marginally consistent with the mass of the IMBH derived dynamically (Gebhardt et al. 2005). Strader et al. (2012a) used deep VLA observations of the globular clusters M 15, M 19 and M 22 to search for radio emission associated with low-level accretion onto an IMBH. No radio sources were detected, putting additional constraints on any IMBH in these globular clusters. Overall, it is probably fair to state that IMBHs have not yet been detected beyond doubt in globular clusters although the evidence for their existence seems to be growing.

Incidentally, in the process of searching for IMBHs in globular clusters, Strader et al. (2012a) *did* find evidence for radio sources in globular clusters albeit not in their cores. The properties of some of these radio sources (flat spectrum radio emission and the limits on/detection of X-ray emission) did provide evidence for the presence of stellar-mass BHs in globular clusters (Strader et al. 2012b; Chomiuk et al. 2013).

5.2 Ultraluminous X-ray sources

Ultraluminous X-ray sources (ULXs) are off-nuclear X-ray point sources in nearby galaxies with X-ray luminosities, $L_X \gtrsim 1 \times 10^{39} - 10^{42} \text{ erg s}^{-1}$ (e.g. Colbert & Mushotzky 1999). Their X-ray luminosities are suggestive of IMBHs if they radiate isotropically at sub-Eddington levels. Hence, ULXs could harbor IMBHs. Alternatively, the radiation in ULXs is not emitted isotropically or the Eddington limit is breached. So called slim disc models could potentially allow for the latter. Below we discuss these possible explanations for the high luminosity in ULXs in more detail.

5.2.1 Beaming and super-Eddington accretion

Relativistic beaming has been proposed as the cause for the high apparent luminosity of ULXs (Körding, Falcke & Markoff 2002). This model predicts that for every high-luminosity source, there should be a larger number of lower luminosity sources; around 30 sources of $L_x \sim 10^{39} \text{ erg s}^{-1}$ for every source of $L_x \sim 10^{40} \text{ erg s}^{-1}$. However, approximately 5-10 sources at $10^{39} \text{ erg s}^{-1}$ are found for each source with luminosity $10^{40} \text{ erg s}^{-1}$ (Walton et al. 2011). As this scenario requires a large number of jet sources beamed in other directions, for which there is no observational evidence it cannot explain the high luminosity for the majority of sources.

Geometrical beaming, where the emission is non-isotropic, provides, in combination with super-Eddington accretion, a viable explanation of the high ULX luminosity. The theory of super-Eddington black hole accretion was developed in the 1980s with the slim disk model of Abramowicz et al. (1980). Here, narrow funnels along the rotation axis of the accretion disk, in part caused by massive radiation-driven winds from the accretion disk, collimate radiation into beams, resulting in an apparent high luminosity as a combination of collimation and super-Eddington accretion rates. Recent simulations support this idea and even with a moderately super-critical mass supply an apparent luminosity $\approx 20 L_{Edd}$ can be reached (Ohsuga & Mineshige 2011). It has also been suggested that strong density inhomogeneities in the accretion disk could cause the escaping flux to exceed the Eddington limit by a factor of $\sim 10 - 100$ (Begelman 2002).

In these models ordinary stellar mass black holes can reach the luminosity observed for most ULXs. However, these scenarios do mean that the Eddington limit is violated and, so far, the Eddington limit works well for almost all known Galactic black holes and AGN (Raimundo et al. 2010). Some Galactic black holes do seem to approach or even breach the Eddington limit, but if so, they do so for only a brief period in time. The conclusion on this issue for Galactic black hole binaries is hampered by the uncertain distance for many sources (Jonker and Nelemans 2004). Of course, perhaps the limited inflow rate is causing the AGNs and most X-ray binaries to remain below the Eddington rate instead of there being a physical barrier at the Eddington limit (Rappaport et al. 2005).

The ULXs with the largest luminosities cannot easily be explained by the geometrical beaming model with super-Eddington accretion rates onto stellar mass black holes unless the mass of these stellar mass black holes is larger than those found in our own Galaxy. The higher the luminosity, the less likely it is that they can be explained as the high-luminosity end of the X-ray binary stellar-mass BH distribution.

A strong case for an IMBH is provided by the variable, very bright ULX ESO 243–49 X–1 (Farrell et al. 2009). Its X-ray luminosity is too high for a stellar-mass black hole even in the presence of some beaming. Given the evidence for the detection of a redshifted $H\alpha$ emission line in the optical counterpart to ESO 243–49 X–1 (Wiersema et al. 2010), the

uncertainty on its distance is reduced with respect to other bright ULXs. Another case for an IMBH is M82 X41.4+60, whereas it does not reach peak luminosities as high as ESO 243–49 X–1, the maximum luminosity is still uncomfortably high for a stellar-mass black hole (Strohmayer and Mushotzky 2003).

Are ULXs really IMBHs or stellar-mass black holes under peculiar accretion conditions? The answer to this question relies on dynamical mass measurements for the black holes in these systems similar to those available for stellar-mass BHs (see Sections 2 and 3). Given the faintness of the optical counterparts (typically $V \geq 22$ mag; see for instance Liu et al. 2004 and Roberts et al. 2008), radial velocity studies of ULXs have concentrated on strong emission lines in the optical spectrum. However, these attempts to provide ULX dynamical masses have not met with success because the emission lines are originating in the accretion disc or a wind, and not in the donor star itself (cf. Liu et al. 2012; Roberts et al. 2011). One potential exception has been mentioned by Liu (2009) who interpret several emission lines as coming from a Wolf Rayet mass donor star to the ULX X–1 in M 101, although no follow-up work has been presented so far.

Searches for photospheric lines have so far concentrated on the blue part of the spectrum as many work on the hypothesis that the donor stars are blue supergiants. This is based on the fact that some ULXs are near a young star cluster and by the blue colours of ULX optical counterparts. However, the blue colours are also consistent with emission from accretion disks as recently has been confirmed by Soria et al. (2012) for a ULX (see also Jonker et al. 2012 and Grisé et al. 2012 for discussions). In fact, it could well be that a significant fraction of the donor stars are red supergiants (Copperwheat et al. 2005; Copperwheat et al. 2007) which are intrinsically bright in the infrared, ($M_V \sim -6$, $V-H \sim 4$, $H-K \sim 0$) in contrast with the blue supergiants ($M_V \sim -6$, $V-H \sim 0$, $H-K \sim 0$). Therefore, some ULX systems may resemble the bright Galactic X-ray binary GRS 1915+105 that has a red giant donor star (Greiner et al. 2001) and thereby radial velocity measurements from infrared photospheric lines will be possible.

From a near-infrared survey of ULX sources within 10 Mpc, Heida et al. (in prep.) found evidence (e.g. see Figure 12) that about 10–15 percent of ULXs have a bright near-infrared counterpart which are consistent with a red-supergiant companion star. However, future near-infrared spectroscopy of these targets should be done to investigate the nature of these near-infrared counterparts.

Acknowledgements We thanks Cristina Zurita, Andrew Cantrell and Rob Hynes for providing us with figures 5, 6 and 11, respectively. JC acknowledges support by the Spanish Ministerio de Economía y Competitividad (MINECO) under grant AYA2010–18080.

References

- M. A. Abramowicz, M. Calvani, L. Nobili, *ApJ* **242**, 772 (1980).
 N. Afshordi, P. McDonald, D. N. Spergel, *ApJ* **594**, L71 (2003).
 M. Armas Padilla, P. N. Degenaar, D.M. Russell, R. Wijnands, *MNRAS* **428**, 3083 (2013a).
 M. Armas Padilla, R. Wijnands, D. Altamirano, M. Méndez, J.M. Miller, N. Degenaar, *MNRAS*, arXiv:1308.4326 (2013b, submitted).
 J.N. Bahcall, R.A. Wolf, *Astrophys. J.* **209**, 214–232 (1976).
 J.N. Bahcall, R.A. Wolf, *Astrophys. J.* **216**, 883–907 (1977).
 C.D. Bailyn, J.A. Orosz, J.E. McClintock, R.A. Remillard, *Nature* **378**, 157 (1995).
 H. Baumgardt, J. Makino, P. Hut, S. McMillan, S. Portegies Zwart, *Astrophys. J. Lett.* **589**, 25–28 (2003).
 G. Beekman, T. Shahbaz, T. Naylor, P.A. Charles, *MNRAS* **281**, L1 (1996).
 G. Beekman, T. Shahbaz, T. Naylor, P.A. Charles, R.M. Wagner, P. Martini, *MNRAS* **290**, 303 (1997).

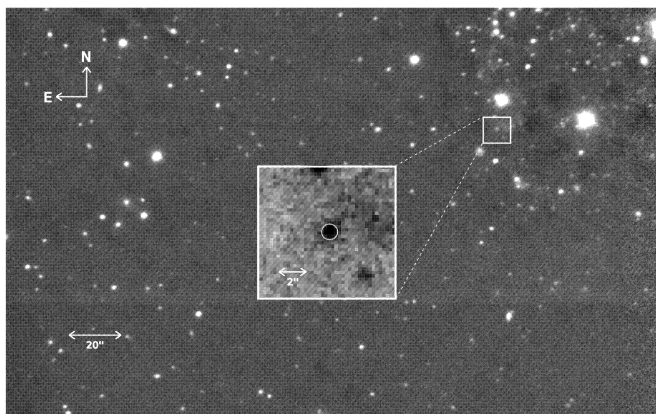


Fig. 12 William Herschel Telescope observations in the Ks-band of the ULX Holmberg II X-1. The small circle indicates the *Chandra* position of the ULX. The inset shows the unique Ks-band counterpart to the ULX (from Heida et al. in prep.).

- M.E. Beer, P. Podsiadlowsky, *MNRAS* **331**, 351 (2002).
M.C. Begelman, *Astrophys. J. Lett.* **568**, 97–100 (2002).
K. Belczynski, T. Bulik, C. L. Fryer, A. Rüter, F. Valsecchi, J. S. Vink, J. R. Hurley, *ApJ* **714**, 1217 (2010).
K. Belczynski, G. Wiktorowicz, C.L. Fryer, D.E. Holz, V. Kalogera, *ApJ* **757**, 91 (2012).
T.M. Belloni, S.E. Motta, T. Muñoz-Darias, *Bull. Astr. Soc. India* **39**, 409 (2011).
C.T. Bolton, *Nature* **235**, 271 (1972a).
C.T. Bolton, *Nature* **240**, 124 (1972a).
C. Brocksopp, A.E. Tarasov, V.M. Lyuty, P. Roche, *A&A* **343**, 861 (1999).
M. Buxton, S. Vennes, *PASP* **18**, 91 (1999).
S.M. Caballero-Nieves et al., *ApJ* **701**, 1895 (2009).
P.J. Callanan, M.R. Garcia, J.E. McClintock, P. Zhao, R. Remillard, F. Haberl, *ApJ* **461**, 351 (1996a).
P.J. Callanan, M.R. Garcia, A.V. Filippenko, I. McLean, H. Teplitz, *ApJ* **470**, L57 (1996b).
D.E. Calvelo, S.D. Vrtilek, D. Steeghs, M.A.P. Torres, J. Neilsen, A.V. Filippenko, J.I. González Hernández, *MNRAS* **399**, 539 (2009).
A.G. Cantrell, C.D. Bailyn, J.E. McClintock, J.A. Orosz, *ApJ* **673**, L159 (2008).
A.G. Cantrell et al., *ApJ* **710**, 1127 (2010).
J. Casares, *IAU Colloq.* **158**, 395 (1996).
J. Casares, *IAU Symp.* **238**, p.3 (2007).
J. Casares, *Ap&SS Proc.*, Springer-Verlag Berlin Heidelberg, p.3 (2010).
J. Casares, P.A. Charles, T. Naylor, *Nature* **355**, 614 (1992).
J. Casares, P.A. Charles, *MNRAS* **271**, 15 (1994).
J. Casares, A.C. Martín, P.A. Charles, E.L. Martín, R. Rebolo, E.T. Harlaftis, A.J. Castro-Tirado, *MNRAS* **276**, L35 (1995a).
J. Casares, P.A. Charles, T.R. Marsh, *MNRAS* **277**, L45 (1995b).
J. Casares, E.L. Martín, P.A. Charles, P. Molaro, R. Rebolo, *NewA* **1**, 299 (1997).
J. Casares, C. Zurita, T. Shahbaz, P.A. Charles, R.P. Fender, *ApJ* **613**, L133 (2004).
J. Casares et al., *ApJS* **181**, 238 (2009).
P.A. Charles, M.J. Coe, *Compact stellar X-ray sources* **39**, p.215 (2006).
A.M. Cherepashchuk, V.M. Lyutiy, R.A. Sunyaev, *Astr.Zh.* **50**, 3 (1973).

- L. Chomiuk, J. Strader, T.J. Maccarone, J.C.A. Miller-Jones, C. Heinke, E. Noyola, A.C. Seth, S. Ransom, arXiv1306.6624 (2013)
- E. J. M. Colbert & R. F. Mushotzky, *ApJ* **519** 89 (1999).
- C. Copperwheat, M. Cropper, R. Soria, K. Wu, "Monthly Notices of the Royal Ast. Society" **362**, 79–88 (2005).
- C. Copperwheat, M. Cropper, R. Soria, K. Wu, "Monthly Notices of the Royal Ast. Society" **376**, 1407–1423 (2007).
- M. Coriat, R.P. Fender, G. Dubus, *MNRAS* **424**, 1991 (2012).
- J.M. Corral-Santana, J. Casares, T. Shabaz, C. Zurita, I.G. Martinez-Pais, P. Rodriguez-Gil, *MNRAS* **413**, L15 (2011).
- J.M. Corral-Santana, J. Casares, T. Muñoz-Darias, P. Rodriguez-Gil, T. Shabaz, C. Zurita, M.A.P. Torres, A. Tyndall, *Science* **339**, 1048 (2013).
- A. Cowley, D. Crampton, G. J.B. Hutchings, R. Remillard, J.E. Penfold, *ApJ* **272**, 118 (1983).
- P.A. Crowther, R. Barnard, G. S. Carpano, J.S. Clark, V.S. Dhillon, A.M.T. Pollock, *MNRAS* **403**, L41 (2010).
- N. Degenaar, R. Wijnands, *A&A* **524**, 69 (2010).
- V.S. Dhillon et al., *MNRAS* **378**, 825 (2007).
- S. Djorgovski, I.R. King, *Astrophys. J. Lett.* **305**, 61–65 (1986).
- H. Falcke, E. Körding, S. Markoff, *Astron. Astrophys.* **414**, 895–903 (2004).
- W.M. Farr, N. Sravan, A. Cantrell, L. Kreidberg, C.D. Bailyn, I. Mandel V. Kalogera, *ApJ* **741**, 103 (2011).
- S.A. Farrell, N.A. Webb, D. Barret, O. Godet, J.M. Rodrigues, "Nature" **460**, 73–75 (2009).
- R.P. Fender et al., *MNRAS* **304**, 865 (1999).
- L. Ferrarese, D. Merritt, *Astrophys. J. Lett.* **539**, 9–12 (2000).
- A.V. Filippenko, T. Matheson, L.C. Ho, *ApJ* **455**, 614 (1995a).
- A.V. Filippenko, T. Matheson, A.J. Barth, *ApJ* **455**, L139 (1995b).
- A.V. Filippenko, T. Matheson, D.C. Leonard, A.J. Barth, S.D. van Dyk, *PASP* **109**, 461 (1997).
- A.V. Filippenko, D.C. Leonard, T. Matheson, W. Li, E.C. Moran, A.G. Riess, *PASP* **111**, 969 (1999).
- A.V. Filippenko, R. Chornock, *IAUC* **7644**, 1 (2001).
- C.S. Froning, E.L. Robinson, *AJ* **121**, 2212 (2001).
- C.L. Fryer, V. Kalogera, *ApJ* **554**, 548 (2001).
- C.L. Fryer, K. Belczynski, G. Wiktorowicz, M. Dominik, V. Kalogera, D.E. Holz, *ApJ* **749**, 91 (2012).
- M.R. Garcia, P.J. Callanan, J.E. McClintock, P. Zhao, *ApJ* **460**, 932 (1996).
- K. Gebhardt, R.M. Rich, L.C. Ho, *Astrophys. J. Lett.* **578**, 41–45 (2002).
- K. Gebhardt, R.M. Rich, L.C. Ho, *Astrophys. J.* **634**, 1093–1102 (2005).
- R.P. Grabhorn, H.N. Cohn, P.M. Lugger, B.W. Murphy, *Astrophys. J.* **392**, 86–98 (1992).
- D.F. Gray, *The Observation and Analysis of Stellar Photospheres*. CUP, Cambridge (1992).
- D.M. Gelino, T.E. Harrison, B.J. McNamara, *ApJ* **122**, 971 (2001a).
- D.M. Gelino, T.E. Harrison, J.A. Orosz, *AJ* **122**, 2668 (2001b).
- D.M. Gelino, T.E. Harrison, *ApJ* **599**, 1254 (2003).
- D.M. Gelino, S. Balman, U. Kiziloglu, A. Yilmaz, E. Kalemci, J.A. Tomsick, *ApJ* **642**, 438 (2006).
- D.R. Gies, C.T. Bolton, *ApJ* **260**, 240 (1982).
- D.R. Gies, C.T. Bolton, *ApJ* **304**, 371 (1986).
- J.I. González Hernández et al., *ApJ* **679**, 732 (2008a).
- J.I. González Hernández, R. Rebolo, G. Israelian, *A&A* **478**, 203 (2008b).
- J.I. González Hernández, J. Casares, *A&A* **516**, A58 (2010).
- J.I. González Hernández, R. Rebolo, J. Casares, *ApJ* **744**, L25 (2012).
- J. Greene, C.D. Bailyn, J.A. Orosz, *ApJ* **554**, 1290 (2001).
- J. E. Greene, L. C. Ho, *ApJ* **670**, 92 (2007).
- J. Greiner, J.G. Cuby, M.J. McCaughrean, *Nature* **414**, 522 (2001).
- J. Greiner, J.G. Cuby, M.J. McCaughrean, A.J. Castro-Tirado, R.E. Mennickent, *Astron. Astrophys.* **373**, 37–40 (2001).
- F. Grisé, P. Kaaret, S. Corbel, H. Feng, D. Cseh, L. Tao *APJ* **745**, 123 (2012).
- E.T. Harlaftis, K. Horne, A.V. Filippenko, *PASP* **108**, 762 (1996).
- E.T. Harlaftis, D. Steeghs, K. Horne, A.V. Filippenko, *AJ* **114**, 1170 (1997).
- E.T. Harlaftis, S. Collier, K. Horne, A.V. Filippenko, *A&A* **341**, 491 (1999).
- E.T. Harlaftis, J. Greiner, *A&A* **414**, L13 (2004).
- C.A. Haswell, E.L. Robinson, K. Horne, R.F. Stiening, T.M.C. Abbott, *ApJ* **411**, 802 (1993).
- A. Herrero, R.P. Kudritzki, R. Gabler, J.M. Vilchez, A. Gabler, *A&A* **297**, 556 (1995).
- R.M. Hjellming, M.P. Rupen, *Nature* **375**, 464 (1995).
- D.J. Hurley, P.J. Callanan, P. Elebert, M.T. Reynolds, *MNRAS* **430**, 1832 (2013).

- J.B. Hutchings, D. Crampton, A. Cowley, *ApJ* **275**, L43 (1983).
- J.B. Hutchings, D. Crampton, A. Cowley, L. Bianchi, I.B. Thompson, *AJ* **94**, 340 (1987).
- R.I. Hynes, D. Steeghs, J. Casares, P.A. Charles, K. O'Brien, *ApJ* **583**, L95 (2003a).
- R.I. Hynes, P.A. Charles, J. Casares, C.A. Haswell, C. Zurita, T. Shahbaz, *MNRAS* **340**, 447 (2003b).
- R.I. Hynes et al., *ApJ* **611**, L125 (2004).
- R.I. Hynes, *ASP Conf. Ser.* **330**, p.237 (2005).
- Z. Ioannou, E.L. Robinson, W.F. Welsh, C.A. Haswell, *ApJ* **127**, 481 (2004).
- P.G. Jonker, G. Nelemans, "Monthly Notices of the Royal Ast. Society" **354**, 355–366 (2004).
- P. G. Jonker et al., *ApJS* **194**, 18 (2011).
- P.G. Jonker, M. Heida, M.A.P. Torres, J.C.A. Miller-Jones, A.C. Fabian, E.M. Ratti, G. Miniutti, D.J. Walton, T.P. Roberts, *ApJ* **758**, 28 (2012).
- S. Kendrew et al., *SPIE* **8446**, 7 (2012).
- J. Khargharia, C.S. Froning, E.L. Robinson, *ApJ* **716**, 1105 (2010).
- J. Khargharia, C.S. Froning, E.L. Robinson, D.M. Gelino *AJ* **145**, 21 (2013).
- P.D. Kiel, J.R. Hurley, *MNRAS* **369**, 1152 (2006).
- A.R. King, U. Kolb, E. Szuszkiewicz *ApJ* **488**, 89 (1997).
- A.K.H. Kong, C.O. Heinke, R. di Stefano, H.N. Cohn, P.M. Lugger, P. Barmby, W.H.G. Lewin, F.A. Primini, "Monthly Notices of the Royal Ast. Society" **407**, 84–88 (2010).
- J.-P. Lasota, *NewAR* **45** 449 (2001).
- E. K rding, H. Falcke & S. Markoff, *A&A* **382** L31 (2002).
- L. Kreidberg, C.D. Bailyn, W. Farr, V. Kalogera, *ApJ* **757**, 36 (2012).
- J.M. Lattimer *ARNPS* **62**, 485 (2012).
- D.T. Larson, E. Schulman, *AJ* **113**, 618 (1997).
- J.-F. Lestrade et al., *A&A* **344**, 1014 (1999).
- J. Liu, *Astrophys. J.* **704**, 1628–1639 (2009).
- J.-F. Liu, J.N. Bregman, P. Seitzer, *Astrophys. J.* **602**, 249–256 (2004).
- J. Liu, J. Orosz, J.N. Bregman, *Astrophys. J.* **745**, 89 (2012).
- L.B. Lucy, *Z.f.Astroph.* **65**, 89 (1967).
- N. L tzingendorf, M. Kissler-Patig, N. Neumayer, H. Baumgardt, E. Noyola, P.T. de Zeeuw, K. Gebhardt, B. Jalali, A. Feldmeier, *Astron. Astrophys.* **555**, 26 (2013).
- P. Madau, M. J. Rees, *ApJ* **551**, L27 (2001).
- T.R. Marsh, E.L. Robinson, J.H. Wood, *MNRAS* **266**, 137 (1994).
- A.C. Martin, J. Casares, P.A. Charles, F. van der Hooft, J. van Paradijs, *MNRAS* **274**, L46 (1995).
- J.E. McClintock, R.A. Remillard, *ApJ* **308**, 110 (1986).
- J.E. McClintock, M.R. Garcia, N. Caldwell, E.E. Falco, P.M. Garnavich, P. Zhao, *ApJ* **551**, L147 (2001).
- J.E. McClintock, R.A. Remillard, *Black Hole Binaries chap.4*, pp.157-213 (2006).
- A. Merloni, S. Heinz, T. di Matteo, "Monthly Notices of the Royal Ast. Society" **345**, 1057–1076 (2003).
- J.C.A. Miller-Jones, P.G. Jonker, V. Dhawan, W. Briskin, M.P. Rupen, G. Nelemans, E. Gallo, *ApJ* **706**, L230 (2009).
- J.C.A. Miller-Jones, J.M. Wrobel, G.R. Sivakoff, C.O. Heinke, R.E. Miller, R.M. Plotkin, R. Di Stefano, J.E. Greene, L.C. Ho, T.D. Joseph, A.K.H. Kong, T.J. Maccarone, *Astrophys. J. Lett.* **755**, 1 (2012).
- M. C. Miller, D. P. Hamilton, *MNRAS* **330**, 232 (2002).
- S. Mineshige, J.C. Wheeler, *ApJ* **343**, 241 (1989).
- I.F. Mirabel, I. Rodrigues, *Science* **300**, 1119 (2003).
- T. Mu oz-Darias, J. Casares, I.G. Mart nez-Pais, *MNRAS* **635**, 502 (2005).
- T. Mu oz-Darias, I.G. Mart nez-Pais, J. Casares, V.S. Dhillon, T.R. Marsh, R. Cornelisse, D. Steeghs, P.A. Charles, *MNRAS* **379**, 1673 (2007).
- T. Mu oz-Darias, J. Casares, I.G. Mart nez-Pais, *MNRAS* **385**, 2205 (2008a).
- T. Mu oz-Darias et al., *AIP Conf Proc.* **984**, p.15 (2008b).
- R. Narayan, J.E. McClintock, *ApJ* **623**, 1017 (2005).
- J. Neilsen, D. Steeghs, S.D. Vrtilik, *MNRAS* **384**, 849 (2008).
- Z. Ninkov, G.A.H. Walker, S. Yang, *ApJ* **321**, 425 (1987).
- K. O'Brien, K. Horne, R.I. Hynes, W. Chen, C.A. Haswell, M.D. Still, *MNRAS* **334**, 4260 (2002).
- D. O'Donoghue, P.A. Charles, *MNRAS* **282**, 191 (1996).
- J.A. Orosz, *ATel* **67** (2001).
- J.A. Orosz, *IAU Symp.* **212**, p.365 (2003).
- J.A. Orosz, C.D. Bailyn, J.E. McClintock, R.A. Remillard, C.B. Foltz, *ApJ* **436**, 848 (1994).
- J.A. Orosz, C.D. Bailyn, *ApJ* **446**, L59 (1995).
- J.A. Orosz, C.D. Bailyn, J.E. McClintock, R.A. Remillard, *ApJ* **468**, 380 (1996).
- J.A. Orosz, C.D. Bailyn, *ApJ* **477**, 876 (1997).

- J.A. Orosz, R.K. Jain, C.D. Bailyn, J.E. McClintock, R.A. Remillard, *ApJ* **499**, 375 (1998).
J.A. Orosz, P.H. Hauschildt, *A&A* **364**, 265 (2000).
J.A. Orosz et al., *ApJ* **555**, 489 (2001).
J.A. Orosz et al., *ApJ* **568**, 845 (2002).
J.A. Orosz, J.E. McClintock, R.A. Remillard, S. Corbel, *ApJ* **616**, 376 (2004).
J.A. Orosz et al. *Nature* **449**, 872 (2007).
J.A. Orosz et al. *ApJ* **697**, 573 (2009).
J.A. Orosz, J.F. Steiner, J.E. McClintock, M.A.P. Torres, R.A. Remillard, C.D. Bailyn, J.M. Miller, *ApJ* **730**, 75 (2011a).
J.A. Orosz, J.E. McClintock, J.P. Aufdenberg, R.A. Remillard, M. Reid, R. Narayan, L. Gou *ApJ* **742**, 840 (2011b).
F. Özel, D. Psaltis, R. Narayan, J.E. McClintock *ApJ* **725**, 1918 (2010).
K. Ohsuga, S. Mineshige, *Astrophys. J.* **736**, 2 (2011).
R.M. O’Leary, A. Loeb, "Monthly Notices of the Royal Ast. Society" **421**, 2737–2750 (2012).
E.P. Pavlenko, A.C. Martin, J. Casares, P.A. Charles, N.A. Ketsaris, *MNRAS* **281**, 1094 (1996).
W. Pietsch et al., *ApJ* **646**, 420 (2006).
Ph. Podsiadlowski, S. Rappaport, Z. Han, *MNRAS* **341**, 385 (2003).
D. Pooley, S. Rappaport, *Astrophys. J. Lett.* **644**, 45–48 (2006).
S.F. Portegies Zwart, S.L.W. McMillan, *Astrophys. J.* **576**, 899–907 (2002).
S.I. Raimundo, A.C. Fabian, F.E. Bauer, D.M. Alexander, W.N. Brandt, B. Luo, R.V. Vasudevan, Y.Q. Xue, "Monthly Notices of the Royal Ast. Society" **408**, 1714–1720 (2010).
S.A. Rappaport, P.C. Joss, in *Accretion Driven X-ray Sources CUP*, 33 (1983).
S.A. Rappaport, P. Podsiadlowski, E. Pfahl, "Monthly Notices of the Royal Ast. Society" **356**, 401–414 (2005).
V. Rashkov, P. Madau, *ApJ*, arXiv1303.3929 (2013, submitted).
M.J. Reid, J.E. McClintock, R. Narayan, L. Gou, R.A. Remillard, J.A. Orosz *ApJ* **742**, 83 (2011).
R.A. Remillard, J.E. McClintock, C.D. Bailyn, *ApJ* **399**, L145 (1992).
R.A. Remillard, J.A. Orosz, J.E. McClintock, C.D. Bailyn, *ApJ* **459**, 226 (1996).
R.A. Remillard, J.E. McClintock, *ARAA* **44**, 49 (2006).
M.T. Reynolds, P.J. Callanan, A.V. Filippenko, *MNRAS* **374**, 657 (2007).
M. Ricotti, J. P. Ostriker, K. J. Mack, *ApJ* **680** 829 (2008).
T.P. Roberts, A.J. Levan, M.R. Goad, "Monthly Notices of the Royal Ast. Society" **387**, 73–78 (2008).
T.P. Roberts, J.C. Gladstone, A.D. Goulding, A.M. Swinbank, M.J. Ward, M.R. Goad, A.J. Levan, *Astronomische Nachrichten* **332**, 398 (2011).
R.W. Romani, *A&A* **333**, 583 (1998).
H. Ritter, A.R. King, *ASP* **261**, 531 (2002).
D. Sanwal et al., *ApJ* **460**, 337 (1996).
M.J. Sarna, *A&A* **224**, 98 (1989).
T. Shahbaz, *MNRAS* **339**, 1031 (2003).
T. Shahbaz, T. Naylor, P.A. Charles, *MNRAS* **268**, 756 (1994a).
T. Shahbaz, F.A. Ringwald, J.C. Bunn, T. Naylor, P.A. Charles, J. Casares, *MNRAS* **271**, L10 (1994b).
T. Shahbaz, F. van der Hooft, P.A. Charles, J. Casares, J. van Paradijs, *MNRAS* **282**, L47 (1996).
T. Shahbaz, T. Naylor, P.A. Charles, *MNRAS* **285**, 607 (1997).
T. Shahbaz, F. van der Hooft, J. Casares, P.A. Charles, J. van Paradijs, *MNRAS* **306**, 889 (1999).
T. Shahbaz, V.S. Dhillon, T.R. Marsh, C. Zurita, C.A. Haswell, P.A. Charles, R.I. Hynes, J. Casares, *MNRAS* **346**, 1116 (2003).
T. Shahbaz, V.S. Dhillon, T.R. Marsh, J. Casares, C. Zurita, P.A. Charles, *MNRAS* **403**, 2167 (2010).
T. Shahbaz, D.M. Russell, C. Zurita, J. Casares, J.M. Corral-Santana, V.S. Dhillon, T.R. Marsh, *MNRAS* **434**, 2696 (2013).
N. Shaposhnikov, L. Titarchuk, *ApJ* **663**, 445 (2007).
J.M. Silverman, A.V. Filippenko, *ApJ* **678**, L17 (2008).
L. Song et al., *AJ* **140**, 794 (2010).
R. Soria, K.D. Kuntz, P.F. Winkler, W.P. Blair, K.S. Long, P.P. Plucinsky, B.C. Whitmore, *Astrophys. J.* **750**, 152 (2012).
D. Steeghs, J. Casares, *ApJ* **568**, 273 (2002).
D. Steeghs, J.E. McClintock, S.G. Parsons, M.J. Reid, S. Littlefair, V.S. Dhillon, *ApJ* **768**, 185 (2013).
J. Strader, L. Chomiuk, T.J. Maccarone, J.C.A. Miller-Jones, A.C. Seth, C.O. Heinke, G.R. Sivakoff, *Astrophys. J. Lett.* **750**, 27 (2012a).
J. Strader, L. Chomiuk, T.J. Maccarone, J.C.A. Miller-Jones, A.C. Seth, "Nature" **490**, 71–73 (2012b).
T.E. Strohmayer, R.F. Mushotzky, *Astrophys. J. Lett.* **586**, 61–64 (2003).

- Y. Tanaka, N. Shibazaki, *ARAA* **34**, 607 (1996).
- M.A.P. Torres, P.J. Callanan, M.R. Garcia, P. Zhao, S. Laycock, A.K.H. Kong, *ApJ* **612**, 1026 (2004).
- M.A.P. Torres et al., *MNRAS* arXiv:1310.02241 (2013, submitted).
- S.C. Unwin, M. Shao, S.J. Edberg, *SPIE* **7013**, 78 (2008).
- J.S. Ulvestad, J.E. Greene, L.C. Ho, *Astrophys. J. Lett.* **661**, 151–154 (2007).
- R.P. van der Marel, in *The Astrophysics of Gravitational Wave Sources*, ed. by J.M. Centrella American Institute of Physics Conference Series, vol. 686, 2003, pp. 115–124.
- F. Valsecchi et al., *Nature* **468**, 7320 (2010).
- A.K.F. Val-Baker, A.J. Norton, I. Negueruela, *AIP* **924**, 530 (2007).
- E.P.J. van den Heuvel, *Proc. Inter. Space Year Conf. ESA ISY-3*, p.29 (1992).
- F. van der Hooft, M.H.M. Heemskerk, F. Albers, J. van Paradijs, *A&A* **329**, 538 (1998).
- J. van Paradijs, J.E. McClintock, X-ray binaries, *Cambridge Astrophysics Series* **26**, p.58 (1995).
- M. Volonteri, *Nature* **466** 1049 (2010).
- M. Volonteri, *Science* **337** 544 (2012).
- R.A. Wade, K. Horne, *ApJ* **324**, 411 (1988).
- R.M. Wagner, T.J. Kreidl, S.B. Howell, S.G. Starrfield, *ApJ* **401**, L25 (1992).
- R.M. Wagner, C.B. Foltz, T. Shahbaz, J. Casares, P.A. Charles, S.G. Starrfield, P. Hewett, *ApJ* **556**, 42 (2001).
- D. J. Walton, T. P. Roberts, S. Mateos, V. Heard, *MNRAS* **416**, 1844 (2011).
- N.A. Webb, T. Naylor, Z. Ioannou, P.A. Charles, T. Shahbaz, *MNRAS* **317**, 528 (2000).
- B.L. Webster, P. Murdin, *Nature* **235**, 37 (1972).
- S. Wellstein, N. Langer, *A&A* **350**, 148 (1999).
- K. Wiersema, S.A. Farrell, N.A. Webb, M. Servillat, T.J. Maccarone, D. Barret, O. Godet, *Astrophys. J. Lett.* **721**, 102–106 (2010).
- M.G. Witte, G.J. Savonije, *A&A* **366**, 840 (2001).
- T-W. Wong, F. Valsecchi, T. Fragos, V. Kalogera, *ApJ* **747**, 111 (2012).
- L.R. Yungelson, J.P. Lasota, G. Nelemans, G. Dubus, E.P.J. van den Heuvel, J. Dewi, S. Portegies Zwart, *A&A* **454**, 559 (2006).
- J. Ziolkowski, *MNRAS* **358**, 851 (2005).
- C. Zurita, et al., *MNRAS* **333**, 791 (2002).
- C. Zurita, J. Casares, T. Shahbaz, *ApJ* **582**, 369 (2003).